Orographically induced flows contributing to convective storm initiation: A review

Robert Kvak[1,2,*], Marek Kašpar[2]

[1] Charles University, Faculty of Science, Department of Physical Geography and Geoecology, Czechia
[2] Czech Academy of Sciences, Institute of Atmospheric Physics, Department of Meteorology, Czechia
[*] Corresponding author: kvak@ufa.cas.cz

ABSTRACT

Mountainous regions worldwide are seasonal hotspots for convective storms. Orographic deep convection is integral to local hydrologic cycles yet poses distinctive natural hazards and remains difficult to forecast, with impacts often extending into adjacent lowlands and densely populated areas. This review synthesizes the current understanding of how terrain-atmosphere interactions and orographically influenced mesoscale flows affect convection initiation (CI) over inland midlatitude complex terrain. The discussion is organized around thermally and mechanically driven processes that control the regional distribution of the three basic CI ingredients, moisture, instability, and lift, with lift being the ingredient most directly modified by mountainous terrain. Under weak synoptic forcing, elevated terrain typically generates thermally driven circulations, whereas stronger background flow forces air to ascend over or divert around topographic barriers. In both regimes, orographic ascent can facilitate CI, especially when combined with terrain-induced modifications of the prestorm thermodynamic environment that enhance low-level moisture and instability. However, convection may be suppressed by shallow cool or stable near-surface layers, persistent intermountain inversions, leeside drying, and mixing by downslope winds, or large-scale warm, dry elevated layers. Orography also exerts a broader regional influence because sufficiently high ranges can modify surface-atmosphere exchange and flow regimes far from the terrain, increasing CI frequency, the propensity for severe weather, and forecast uncertainty. The paper highlights the need for future meso- and microscale research in mountain environments to improve the understanding of CI distributions and their associated societal impacts.

KEYWORDS

convection initiation; orographic processes; prestorm thermodynamics; mesoscale flows; mountain meteorology

Received: 15 December 2025
Accepted: 9 April 2026
Published online: 30 April 2026

Kvak, R., Kašpar, M. (2026): Orographically induced flows contributing to convective storm initiation: A review, e23361980.2026.7
https://doi.org/10.14712/23361980.2026.7

1. Introduction

Convective storms are formally defined by the occurrence of deeply developed cumulonimbus clouds that produce precipitation (AMS 2025; CMeS 2025). In the literature, various terms are used to describe such phenomena, often referring to the same process of deep moist convection driven by buoyancy (Markowski and Richardson 2010). In this review, expressions including deep convection, thunderstorm, or simply storm are used synonymously, while recognizing that not every convective storm produces lightning and that such storms do not necessarily occur as part of a larger synoptic-scale storm system (Doswell 1987; Doswell 2001; Doswell and Bosart 2001). A similar principle of terminological flexibility, applied without strict distinction throughout this paper, extends to terrain-related features that may, according to their natural significance or origin, be referred to as mountains, hills, orography, topography or complex terrain, depending on regional or disciplinary conventions (e.g., Price et al. 2019).

All convective storms require three atmospheric preconditions for their initial growth: (1) a sufficient volume of moist air that is relatively warm, (2) an adequately decreasing temperature with height that allows this air to ascend, and (3) a mechanism that provides the initial lift for the air (Doswell et al. 1996). This fundamental set of ingredients applies to the initiation of every type of convective storm, including single cells, multicells, and supercells, but the persistence and organization of more complex storms or larger convective systems also depend on environmental wind shear (Weisman and Klemp 1982). Because storm organization is not the focus here, we refer readers to the relevant literature (e.g., Markowski and Dotzek 2011; Miglietta and Rotunno 2014; Soderholm et al. 2014; Mulholland et al. 2018; Ammon et al. 2025; Riggin et al. 2025).

The foregoing preconditions arise from surface-atmosphere exchanges of heat, moisture, mass, and momentum, so changes in surface properties inherently modify the prestorm environment (Kang and Ryu 2016; Kirshbaum et al. 2018; Schneider et al. 2018). For several decades, research has examined how mountainous terrain alters these environments and whether such influences promote or hinder convective storm development, an issue highlighted early by Banta (1990) in the textbook edited by Blumen (1990). By that time, it was already recognized that orography can provide crucial initial lift for moist air on scales smaller than synoptic ascent, which is typically too weak to initiate deep convection (Doswell 1987). It was also understood that basic processes over elevated terrain can modify temperature and dewpoint lapse rates and the wind field relative to lower elevations (e.g., Houze et al. 1993). However, a more integrated picture of how mountainous terrain modifies prestorm environments and influences deep convection initiation remained comparatively limited.

Some studies (e.g., Barthlott et al. 2010; Weckwerth et al. 2011; Khodayar et al. 2013; Davolio et al. 2016) confirmed and expanded earlier knowledge by showing that the primary and strongest sources of orographically induced environmental modification stem from two broader groups of mesoscale effects, described by De Wekker and Kossmann (2015) as active and passive. These effects comprise (1) differential heating of sloping terrain, which generates thermally driven temperature and pressure perturbations, and (2) interactions between elevated terrain and the larger-scale airflow, which produce mechanically forced pressure anomalies. Resulting mesoscale circulations and flow perturbations can cause coherent ascent or descent of air masses and transport heat and moisture, leading to localized anomalies in vertical motion, temperature, and moisture distribution (Kirshbaum et al. 2016; Kirshbaum and Schultz 2018; Reif and Bluestein 2018; Nelson et al. 2021, 2022).

This review focuses specifically on these mesoscale atmospheric processes, described by Doswell (2001) as forced and external during the initiation of convective storms (hereafter CI), and which range in scale from a few to several hundred kilometers (Markowski and Richardson 2010). Because they exist regardless of the various surface characteristics present (for example, bare rock or vegetation), they are collectively referred to as orographic (De Wekker et al. 2018). These processes operate across a wide range of terrain scales, from minor coastal asymmetries to high alpine peaks, and their spatial extent, magnitude, and regime vary considerably among different landforms (e.g., Hilel Goldshmid et al. 2018), climatic regions (e.g., Nicolas and Boos 2022), and synoptic patterns (e.g., Schultz et al. 2025). Some of these processes may also occur in winter (e.g., Afrifa et al. 2025), and over coastal areas, where additional mechanisms such as land-sea breezes can favor CI (e.g., Kirshbaum et al. 2016).

The coverage of this paper is limited to midlatitude inland regions and primarily to the warmer months, when deep convection is most frequent. During the European warm season, ten-year satellite analyses have shown that CI tends to intensify on the lee sides of major mountain ranges (Levizzani et al. 2010), including the Alps, Apennines, Atlas Mountains in North Africa, Carpathians, Pyrenees, and the mountains of the Balkan Peninsula. Less direct but complementary evidence from lightning observations confirms that these mountains experience the highest seasonal frequencies of lightning-producing storms (e.g., Battaglioli et al. 2023). Fig. 1 presents results from Taszarek et al. (2019), demonstrating that some of those areas exhibit, on average, up to about 40 thunderstorm days per warm season. Similar mountain-enhanced lightning activity is also evident in global data (e.g., Peterson et al. 2021). Within Europe, climatological studies

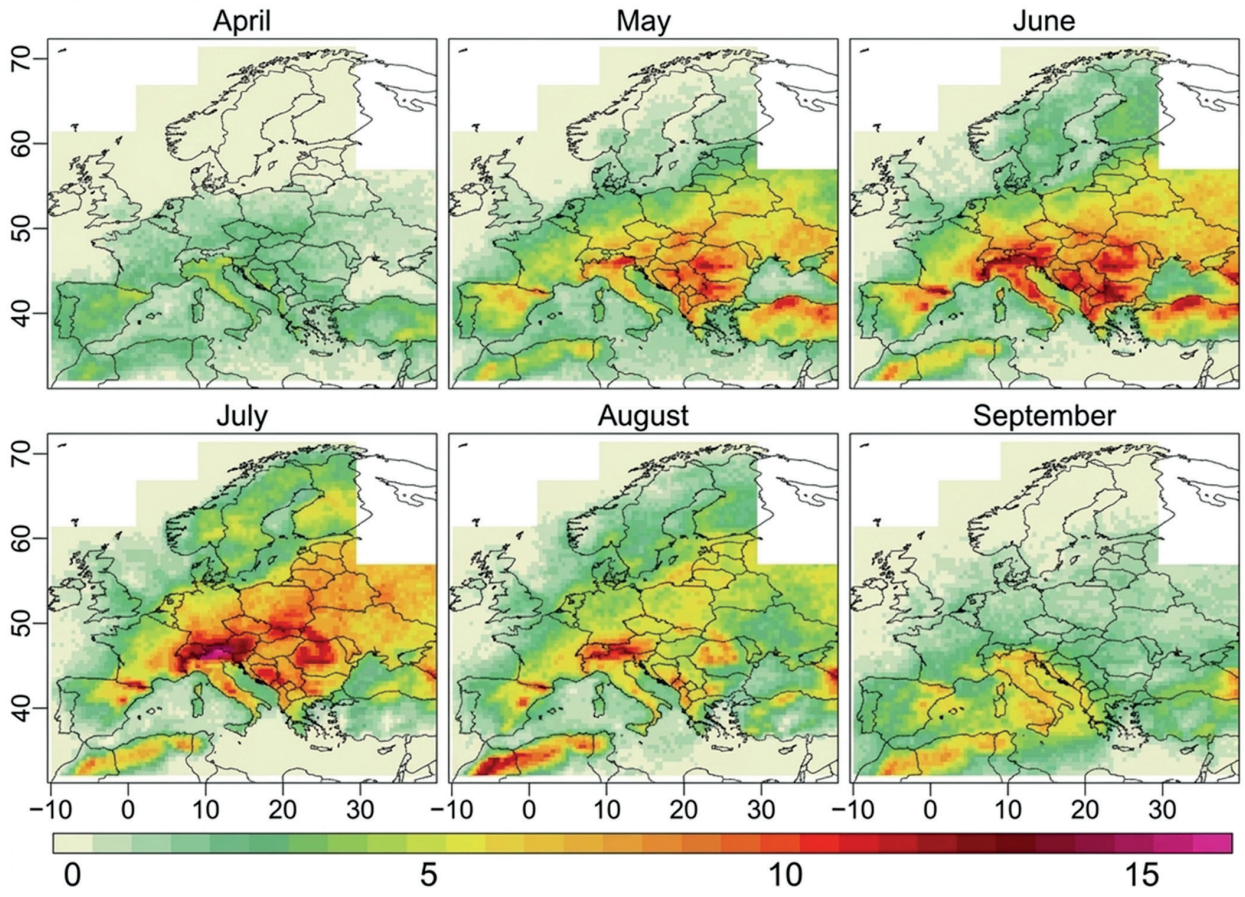

Fig. 1 Monthly (April–September) mean number of days with thunderstorms over Europe based on lightning data from the EUCLID and ZEUS networks. A thunderstorm day is defined as one with more than two lightning flashes within a 0.5° × 0.5° grid cell, which corresponds to roughly 55 km in the north-south direction and 25–45 km in the east-west direction. Figure reproduced from Taszarek et al. (2019, their Fig. 4) with permission.

of convective precipitation (e.g., Lombardo and Bitting 2024), hail (e.g., Punge and Kunz 2016), and other hazardous convective weather and associated environments (e.g., Taszarek et al. 2020a, b) are consistent with these findings.

Because higher storm frequency implies higher exposure, mountainous regions can be disproportionately vulnerable. Narrow valleys, especially in arid, sparsely vegetated mountains, can function as runoff channels, producing localized flash floods (e.g., Panziera et al. 2015), while heavy rainfall on steep terrain and saturated soils can initiate landslides and destructive debris flows (e.g., Bačová Mitková et al. 2018). An enhanced occurrence of large-hail events in the vicinity of mountains can result in frequent injuries to people and animals and severe damage to agriculture (e.g., Trefalt et al. 2018), whereas severe winds may break branches, uproot trees, or cause other impacts in terrain-induced exposure zones (e.g., Frame and Markowski 2006). Additionally, elevated lightning activity poses direct dangers to individuals engaged in recreational activities (e.g., Kühne et al. 2025) and can also trigger secondary hazards such as wildfires (e.g., Rorig and Ferguson 1999).

Public risk perception often underestimates the frequency of convective storms and their associated hazards, and not only in mountains (Doswell 2015; Brooks et al. 2019). Moreover, numerical weather prediction models continue to struggle with forecasting convective storms over complex terrain (e.g., Rotach et al. 2022; Fischer et al. 2025), and operational forecasters face even greater challenges when interpreting weather patterns in mountainous regions (e.g., Barrett et al. 2015; Groenemeijer et al. 2017). Consequently, the public may rely on vague forecasts, misunderstand the communicated information, or, in the worst cases, disregard the forecast altogether.

Motivated by these challenges, this review provides a process-based synthesis and conceptual framework for a broad Earth-science readership, including students and early-career researchers, focused on mesoscale orographic processes that shape the pre-storm environment and contribute to CI. This topic is often treated only briefly in broad Earth-science overviews, despite its relevance for warm-season hazards in some regions. In addition to summarizing the literature, the paper frames terrain-driven CI mechanisms through an ingredients lens and highlights key knowledge gaps. The manuscript is not intended as an operational forecasting guide and does not attempt a comprehensive synoptic classification or case-study approach.

The review is organized around thermally driven and mechanically forced mesoscale flows, interpreted through their impacts on the three CI ingredients (moisture, instability, and lift). Section 2 summarizes key characteristics of mountainous convective environments, emphasizing the vertical structure of instability. Sections 3 and 4 review CI mechanisms linked to thermally driven and mechanically forced flows, respectively. Section 5 summarizes the main findings and closes with directions for future work.

2. Overview of prestorm thermodynamics in mountain environments

In mountainous environments, mesoscale orographic processes modify the prestorm environment by redistributing boundary-layer moisture and heat and by generating mesoscale convergence and ascent, thereby contributing to CI. These processes can often be grouped into two dominant forcing pathways: (1) thermally driven circulations that promote buoyancy and convergence, and (2) mechanically forced ascent associated with terrain-flow interaction (Lareau et al. 2024). Although this split is a useful organizing framework, many real cases involve concurrent thermal and mechanical contributions that are difficult to separate observationally. For successful CI, both initiation pathways ultimately require conditional instability, meaning that the environmental temperature lapse rate (Γ) lies between the moist-adiabatic lapse rate ($\Gamma_s \approx 2$–9 K km^{-1}) and the dry-adiabatic lapse rate ($\Gamma_d \approx 9.8$ K km^{-1}), allowing saturated air parcels to accelerate upward and produce deep vertical motions (Doswell 2001; Kirshbaum et al. 2018).

Most environments with conditional instability are created by large-scale circulations (Doswell 1987; Doswell and Bosart 2001; Roe 2005), whereas orographic effects reshape how that instability is realized as CI (Houze 2012; Katona et al. 2016). While evidence for systematic terrain-driven changes in instability is robust, their translation into CI outcomes can vary widely with the depth of the moist layer, cloud-layer entrainment, and background forcing. Overall, sloped terrain exposed to solar radiation warms more rapidly and can steepen the near-surface Γ. This steepening may be limited by weaker surface heating over bright land cover, colder water bodies, vegetation, snow cover, or glaciers (e.g., De Wekker and Kossmann 2015; Ammon et al. 2025). In contrast, during nighttime, inversions of air temperature (T) commonly form in valleys and basins, leading to strong static stability (Whiteman 2000).

In addition to instability, sufficient low-level humidity is essential for the development of positively buoyant updrafts. This is challenging in mountainous regions, where specific humidity generally decreases with height and air masses at higher elevations are typically much drier than near the surface (Barry 2008). Nevertheless, Fig. 1 and several observational studies (e.g., Weckwerth et al. 2011; Lock and Houston 2015; Feldmann et al. 2021) show that CI occurs more frequently over hilly or mountainous terrain than over flat plains, implying that moisture is transported upslope by flows that enhance low-level convergence or is supplemented by local evaporation (e.g., Hassanzadeh et al. 2016). As a result, low-level air over mountains can become more humid, and correspondingly warmer, than the surrounding free atmosphere at the same elevation, promoting enhanced moist destabilization (Imamovic et al. 2019). The vertical depth and persistence of this moist anomaly remain uncertain and can differ substantially between enclosed basins, open valleys, and exposed ridgelines. This behavior was documented by Kelsey et al. (2018) in the northeastern United States, although they noted that humidity at the summit remained lower than within roughly the lowest 560 m above ground level (AGL) in the nearby valley.

Higher near-surface humidity, represented by the dewpoint T_d, together with soil moisture, vegetation, and nearby water bodies, can reduce the daytime Γ by enhancing evaporative cooling, which limits sensible heat fluxes, turbulent mixing, and moist convective circulations (Barthlott and Kalthoff 2011). Nonetheless, several studies (e.g., Laiti et al. 2014; Imamovic et al. 2017; Feldmann et al. 2024) show that increased water-vapor content can also strengthen local circulations and convective updrafts. Imamovic et al. (2017) found that the sensitivity of precipitation totals to soil moisture decreases with increasing mountain elevation and that soil-moisture effects are overwhelmed by thermally driven circulations once terrain exceeds roughly 500 m. In addition, localized heat sources such as wildfires can trigger deep convection in some settings, even without enhanced low-level moisture (e.g., Peterson et al. 2017).

Given sufficient instability and moisture, an air parcel lifted by orographic influence or other mechanisms cools dry adiabatically until it reaches the lifting condensation level (LCL), where it becomes saturated and further ascent produces condensation and cloud formation (Houze 1993). In more humid mountainous regions, such as central Europe, LCLs in both nonsevere and severe storm environments are typically near or below 1000 m AGL, whereas in drier regions such as central Argentina, they more often exceed 1000 m during CI (e.g., Púčik et al. 2015; Mulholland et al. 2018; Taszarek et al. 2020b; Lareau et al. 2024). Across studies, LCL height appears more influential for severe-storm character than for nonsevere convection. Mulholland et al. (2019) linked higher LCLs in high-terrain experiments to stronger supercell downdrafts, and Púčik et al. (2015) suggested that higher LCLs may support more persistent, broader updrafts conducive to large hail.

For moist air to accelerate upward and reach CI, it must be lifted from below the LCL to the level of

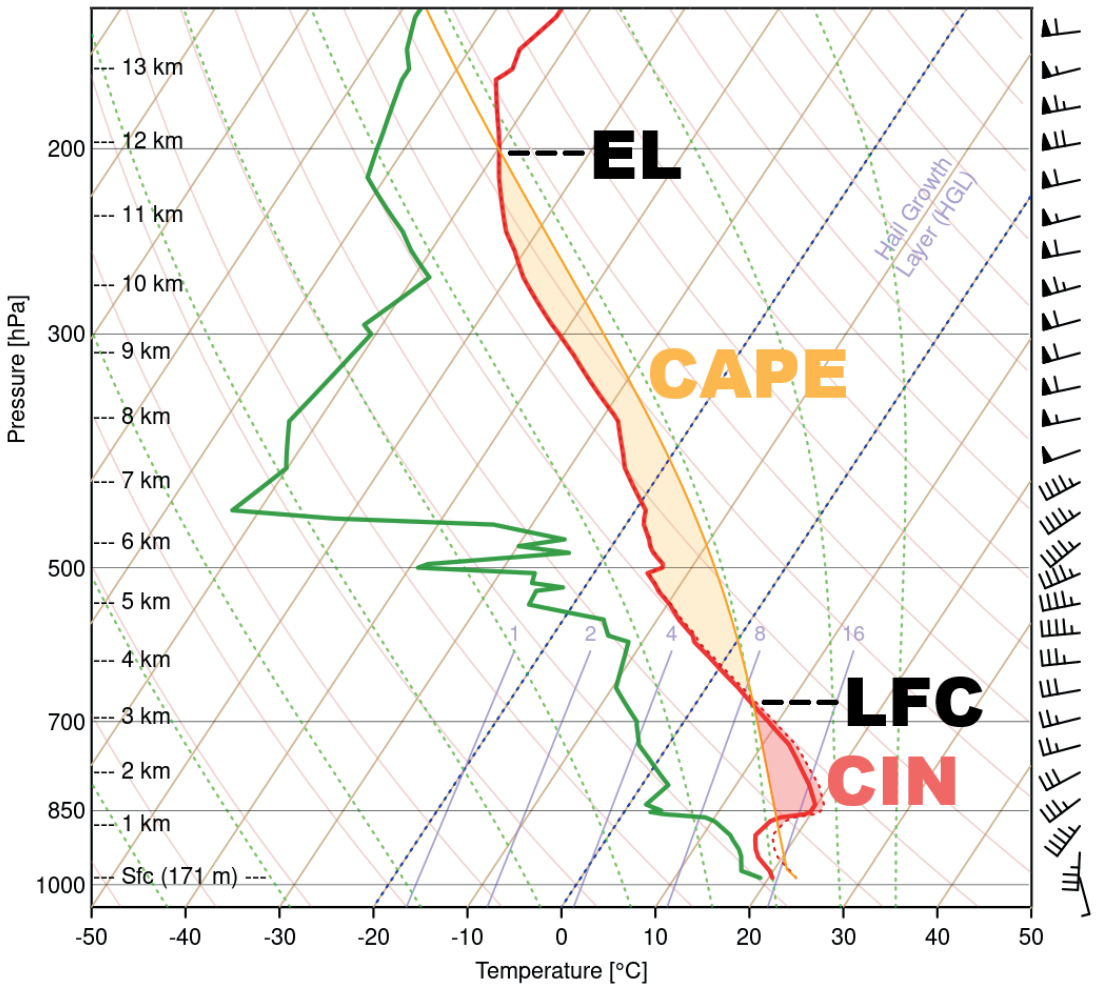

Fig. 2 Skew *T*-log *p* diagram from an atmospheric radiosonde launched at 1200 UTC 9 April 2015 from Fort Worth, Texas (USA). Environmental temperature (solid red) and dewpoint (solid green) profiles are shown with pressure and height AGL on the left vertical axis, and wind barbs on the right. The dashed red curve denotes the environmental virtual temperature profile, which is used together with the virtual temperature of the lifted air parcel (yellow curve) to compute LFC, equilibrium level (EL), CAPE, and CIN. The physically meaningful LFC above the temperature inversion (above 1 km AGL) and the EL are marked for a surface-based parcel. The yellow-shaded area represents CAPE, and the red-shaded area below the LFC represents CIN. For further details on the diagram, see, for example, Markowski and Richardson (2010, pp. 15 and 34). Figure generated using the *thundeR* software (Czernecki et al. 2025).

free convection (LFC), where it becomes warmer than the environment, and buoyancy becomes positive. Enhanced vertical motions provided by orographic lifting are often crucial for successful CI (e.g., Nelson et al. 2021; Marquis et al. 2023). Without sufficient lift, other mesoscale processes are unlikely to initiate convection, and CI frequently fails (e.g., Lock and Houston 2014; Smith et al. 2015). Observation-based studies in South America (Marquis et al. 2021; Feng et al. 2022; Nelson et al. 2022) further showed that free-tropospheric humidity strongly modulates CI, with entrainment of dry air limiting updraft depth, buoyancy and storm lifetime. In practice, near-cloud thermodynamics are rarely sampled well enough to attribute CI success or failure to the local moisture and stability field. Fig. 2 summarizes the thermodynamic controls on CI: convective available potential energy (CAPE) quantifies how strongly an updraft can accelerate once convection becomes buoyant, whereas convective inhibition (CIN) quantifies the cap that resists parcel ascent and can prevent initiation.

Steeper Γ combined with higher low-level T_d increases instability and CAPE while reducing CIN. Over higher terrain, however, CAPE and storm frequency are often lower because near-surface air is cooler and drier and the vertical depth available for ascent is reduced (e.g., Panosetti et al. 2016; Feldmann et al. 2021). Mountains can still enhance CAPE locally through stronger surface heating and modified low-level moisture flows (Chen and Lin 2005; Kirshbaum 2013; Panziera et al. 2015). For example, climatological studies such as Katona et al. (2016) and Taszarek et al. (2020b) show, in addition to a latitudinal dependence of prestorm CAPE, clear orographic signatures along major ranges. CIN decreases when enhanced heating on sunlit slopes steepens the low-level Γ and increases T_d locally (e.g., Scheffknecht et al. 2017). By contrast, CIN increases when stable layers develop in valleys at night, when cold-air pools or downslope flows strengthen near-surface stability, or when dry, warm air aloft overlies moist boundary-layer air and reinforces a capping inversion (Doswell and

Bosart 2001; Degiacomi et al. 2025). These contrasts underscore that the effective CAPE and CIN influencing CI in complex terrain can remain poorly constrained, because initiating parcels sample a highly heterogeneous near-surface thermodynamic field.

Although conditional instability provides the basic thermodynamic support for deep convection, other mesoscale instability types can also aid CI. Potential instability arises when equivalent potential temperature (θ_e) decreases with height and mechanical lift releases latent heat from moist lower layers beneath cooler, drier air aloft (Řezáčová et al. 2007; Afrifa et al. 2025). Some studies (e.g., Kaspar et al. 2009; Wulfmeyer et al. 2011; Tang et al. 2016; Kunz et al. 2018) have linked this instability to severe storm development near mountains, where it can be released by terrain-forced lifting. This configuration commonly occurs when daytime heating over mountains steepens Γ and advection of the destabilized air over more humid boundary-layer air forms an elevated mixed layer (EML; Reif and Bluestein 2018; Schultz et al. 2025). Fig. 2 illustrates such an environment in Texas, with an EML near 850 hPa characterized by higher T and lower T_d and southwesterly flow aloft from the central Mexican Plateau, while south-southeasterly low-level winds beneath the inversion transport moist air from the Gulf of Mexico.

To conclude this section, and paraphrasing Markowski and Richardson (2010, p. 188), in mountain environments, both CAPE and CIN can be modified on the mesoscale by three categories of processes that arise from surface-atmosphere interactions. They can be enhanced and reduced, respectively, by (1) thermally driven circulations resulting from warming on sunlit slopes, (2) mechanically forced ascent around terrain barriers, and (3) low-level moistening through moisture advection or evapotranspiration. These changes can arise from warming or moistening alone, without requiring large changes in Γ. The following sections emphasize the first two categories, consistent with the CI mechanisms summarized by Houze (1993, 2012), because they most directly generate mesoscale convergence and ascent while redistributing heat and moisture. This separation also reflects their contrasting controls: thermally driven circulations are most prominent under weak background flow and strong diurnal heating, whereas mechanically forced ascent is favored under stronger ambient flow and depends primarily on upstream stability and terrain geometry.

3. Thermally driven orographic circulations

Solar radiation drives the surface-atmosphere energy balance and the vertical temperature stratification that governs atmospheric stability and the potential for CI. Thermally induced orographic circulations contribute to CI by generating mesoscale convergence and ascent while also redistributing boundary-layer moisture and modifying CAPE and CIN. Their effectiveness therefore depends on the presence (or local enhancement) of sufficiently moist, conditionally unstable air. During the diurnal cycle, solar-driven surface turbulent heat fluxes generate buoyant thermals of various sizes and magnitudes that strongly depend on the intensity of solar insolation and thus on latitude and altitude, season, solar elevation angle, aspect and slope of terrain, and shading by clouds or nearby terrain, and also on land cover (e.g., Serafin and Zardi 2010; Kirshbaum 2017; De Wekker et al. 2018; Serafin et al. 2018; Ammon et al. 2025). Accordingly, thermally driven circulations are most effective under weak background flow, when diurnal heating can organize persistent convergence that lifts parcels toward their LFC. The east-west progression of diurnal heating in the Northern Hemisphere also shifts surface-based buoyancy and inhibition across opposing slopes and interacts with smaller-scale thermals (e.g., Kottmeier et al. 2008).

Sensible heat flux drives shallow convective boundary-layer (CBL) updrafts of 0.1–1 m s^{-1} and, over well-heated hilly terrain, can produce vertical velocities of several m s^{-1} (Kirshbaum and Wang 2014; Panosetti et al. 2016). Even vertical velocities near 10 cm s^{-1} can help lift air parcels toward saturation, reduce CIN, and promote CI in environments already close to instability (Doswell and Bosart 2001). These thermally driven motions shape the CBL and often initiate early convective clouds within low-level convergence zones and surface thermal hot spots, most prominent on cloudless summer days (e.g., Bianco et al. 2011; Imamovic et al. 2019). Nelson et al. (2022) showed that terrain-enhanced lift can allow CI to develop from boundary-layer thermals that are more than twice as narrow as those required without terrain forcing (~1–2 km versus ~5 km). A persistent challenge is that storm-scale convergence and near-CI updraft structure are highly localized and short-lived, and are therefore difficult to observe and attribute in complex terrain (e.g., Marquis et al. 2023).

Since complex elevated terrain typically undergoes stronger diabatic heating and cooling than surrounding lower elevations, the resulting solar- and terrain-driven temperature and pressure gradients (∇T and ∇p) generate persistent solenoidal and baroclinic circulations from local to mountain range scales once low-level stability is eroded (e.g., Doswell 2001; Barthlott et al. 2006; Wagner et al. 2015). Conceptual models (e.g., Barry 2008; Chow et al. 2013) typically categorize five such orographic circulations based on the size, landform, diurnal phasing, and flow strength: slope winds, valley winds, plateau winds, basin winds, and mountain-plain circulations. Fig. 3 shows that the diurnal cycle of each circulation reflects the local ∇T and ∇p, with two main phases: daytime flow from lower to higher elevations and nighttime flow from higher to lower elevations, separated by transition periods.

Crucially, each circulation occupies a different layer AGL, and its transition phases are shifted relative to the others, with the timing depending on the distance from the landform that generates it (e.g., Graf et al. 2016).

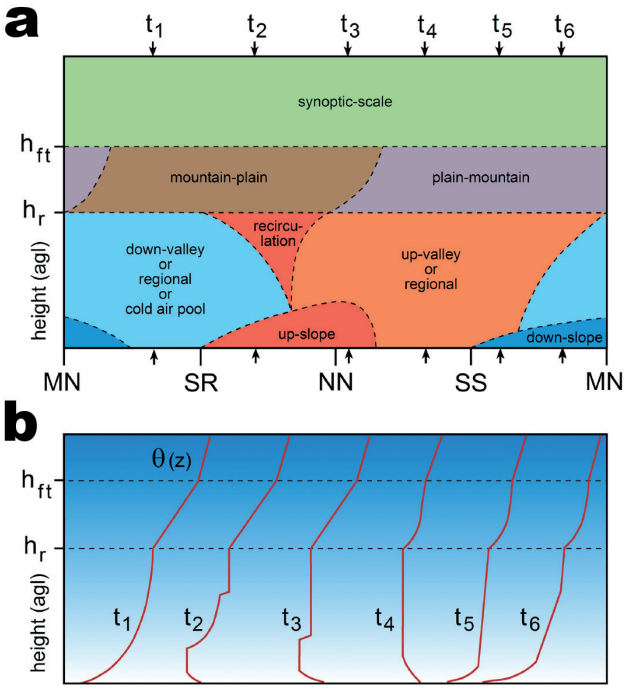

Fig. 3 Diurnal mountain circulations and boundary-layer structure over a slope. (a) The panel illustrates prevailing mountain circulations and their transition phases (dashed lines) as a function of time (MN for midnight, SR for sunrise, NN for noon, and SS for sunset) and height above the mountainside. The levels h_r and h_{ft} indicate the ridge-top height and the base of the free troposphere outside the mountain atmosphere. (b) The panel shows the diurnal evolution of potential-temperature profiles $\vartheta(z)$ above slopes (t_1 to t_6), with the timing of each profile marked by small arrows in panel (a). Figure reproduced from De Wekker and Kossmann (2015, their Fig. 3) with permission.

These mountain circulations are most efficient under clear skies, weak low-level stability, and mild synoptic background flows, although the threshold at which weak background flow transitions to a regime where thermal circulations are disrupted remains difficult to generalize (e.g., Hagen et al. 2011; Khodayar et al. 2013; Kirshbaum 2013; Bergmaier and Geerts 2015; Scheffknecht et al. 2017). Consequently, relatively dry and complex terrain enhances thermal circulations and increases the likelihood of CI (Banta 1990; Damiani et al. 2008; Imamovic et al. 2017). Despite this, very dry regions may lack adequate low-level moisture, limiting deep convection unless elevated mountains ventilate the CBL with additional moisture from the free troposphere, producing local θ_e maxima. Additionally, thermal circulations become weakened by vast reflective, cool or moistened surfaces, when ∇T and ∇p diminish, and the near-surface vertical gradient of potential temperature ($\partial\theta/\partial z$) becomes strongly positive (Imamovic et al. 2019). Under strong ambient winds, thermal circulations can be partly masked, yet they generally persist even if difficult to observe directly (e.g., De Wekker et al. 1998; Barthlott et al. 2010; Wagner et al. 2015; Kelsey et al. 2018).

3.1 Airflow over mountain slopes

Slope winds are the fundamental component of thermally driven circulations in mountainous terrain. Slope aspect, angle, and surface properties control the thermal forcing that drives local slope flows and, in turn, larger valley and mountain-plain circulations (Fig. 3a). During daytime, anabatic winds develop along heated slopes, accompanied by weak compensating return flows aloft, and can form paired opposing circulations when present on both sides of a valley (Fig. 4). These

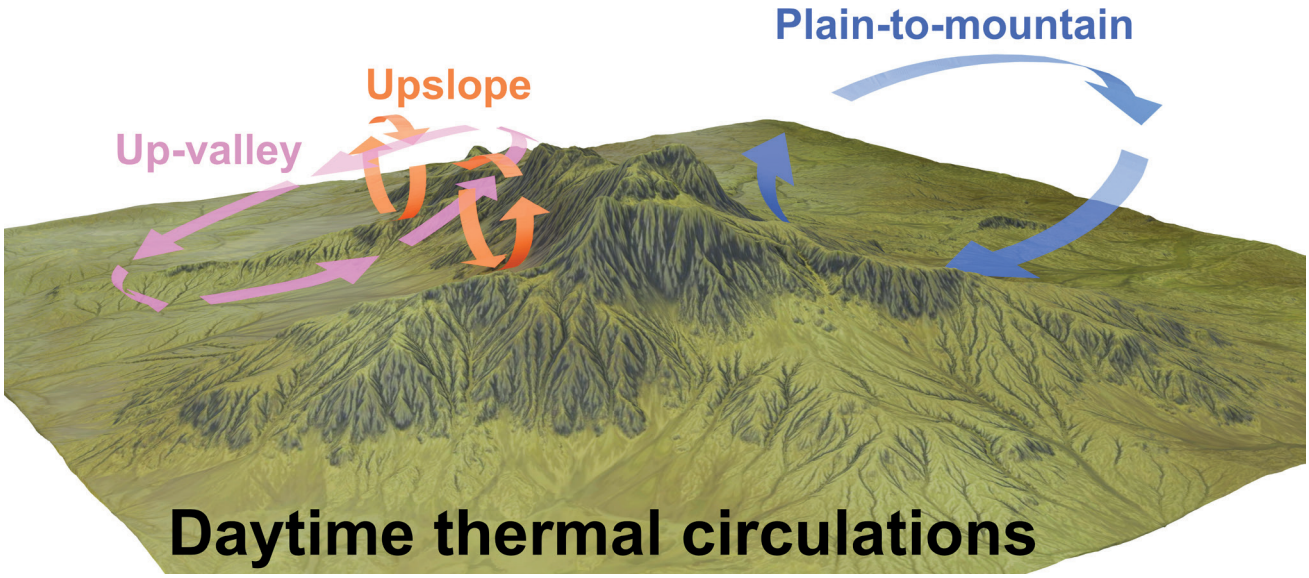

Fig. 4 Three interacting thermally driven wind systems over mountainous terrain during daytime. The upslope flows on the valley sidewalls oppose each other and are accompanied by subsidence over the valley center. Similar upslope flow also develops outside the valley along the surrounding foothills. The up-valley flow extends from the valley mouth toward the valley head and may be crossed by a cross-valley circulation that transports air from cooler to warmer sidewalls (not shown). The plain-to-mountain flow is the spatially largest system and transports air from the adjacent plain toward the mountain thermal low. Figure drafted by Miroslav Truben in collaboration with the authors.

buoyancy-driven flows typically reach 1–5 m s^{-1}, occupy roughly the lowest 200 m AGL, and are strongly damped by surface friction (e.g., Chow et al. 2013; Serafin and Zardi 2010). Daytime solar heating produces a near-surface superadiabatic layer with $\partial\theta/\partial z < 0$ (profiles t_2–t_4 in Fig. 3b), which promotes buoyant instability, strengthens upslope flow, and favors convergence zones along sun-exposed slopes where air is forced to ascend (Barthlott et al. 2006).

Under fair-weather conditions, the strongest surface heat fluxes, converging upslope flows, moistening, and resulting orographic ascent occur over the highest terrain and along ridge crests (e.g., Kottmeier et al. 2008). This forcing warms and deepens the CBL and destabilizes the air near ridge-top level (profiles t_4–t_6 in Fig. 3b), producing local CIN minima over elevated peaks (e.g., Kalthoff et al. 2011; Bergmaier and Geerts 2015). Fig. 5a illustrates the first initiation mechanism, in which thermally driven lift within these exposed thermal hot spots enhances the likelihood for CI. Strong contrasts in upslope wind strength, CAPE, and CIN often exist between sunlit and shaded slopes. In the Northern Hemisphere, south-facing slopes receive greater solar input and are therefore more favorable for thermal hot spot formation (e.g., Panziera et al. 2018). Idealized simulations by Hassanzadeh et al. (2016) indicate that CI may occur relatively early in the morning in the lee of a mountain when thermal upflow interacts and converges with the background wind.

Numerical simulations by Imamovic et al. (2019) showed that upslope winds are essential for transporting moist, conditionally unstable air toward thermal hot spots and, under even weak background flow oriented perpendicular to the main mountain range, can carry this air beyond complex ridge systems. Their results also demonstrated that mountain geometry strongly modulates moisture transport. Narrower, taller mountains produce stronger upslope winds but draw from a smaller CBL volume and therefore transport less total moisture, whereas wider, lower mountains generate weaker winds yet interact with a larger reservoir of near-surface air and convey more moisture. The taller mountains, however, tend to produce the strongest summit moisture anomalies. Such geometric contrasts may influence the location of CI. For example, Bergmaier and Geerts (2015) suggested that particularly high mountain ranges can act as natural barriers to mesoscale moist upslope flows and inhibit CI over adjacent terrain.

After sunset, radiative surface cooling generates a stable near-surface layer that initiates katabatic downslope winds that are slightly weaker than their daytime anabatic counterparts (Fig. 3a). In this regime, $\partial\theta/\partial z > 0$ dominates the vertical profile (Fig. 3b), producing a low-CAPE, high-CIN environment in which deep convection is usually suppressed, especially over mountain crests and higher slopes. Only later in the night may higher terrain protrude above the deepening nocturnal inversion over lower elevations, reducing its stabilizing influence. Downslope winds can nevertheless interact with background or locally moist low-level flows over adjacent plains, as observed along the Rockies and Andes (e.g., Friedrich et al. 2016; Mulholland et al. 2018; Reif and Bluestein 2018; Singh et al. 2022), where such interactions contributed to the evolution of convergence zones capable of providing sufficient lift for CI (Fig. 5b). This mechanism is favored when downslope winds strengthen under weak ambient flow and stability (e.g., Kirshbaum and Wang 2014).

Radar analysis by Kaltenboeck and Steinheimer (2015) showed that lightning activity often propagates off the mountains into the Alpine foreland during the evening and early night. Consistently, Taszarek et al. (2020a) found that mean annual nighttime lightning over land maximizes in relatively flat lowland regions, including the northern Great Plains and Columbia Plateau in the United States and the Pannonian Basin and North European Plain in Europe. Although environmental stability increases at night, secondary nocturnal CI can be as strong as daytime initiation, and mountain convection can act as a precursor to subsequent lowland CI (Chow et al. 2013). These patterns suggest organized lifting, but the mechanisms controlling the timing and preferred mountain-to-plain

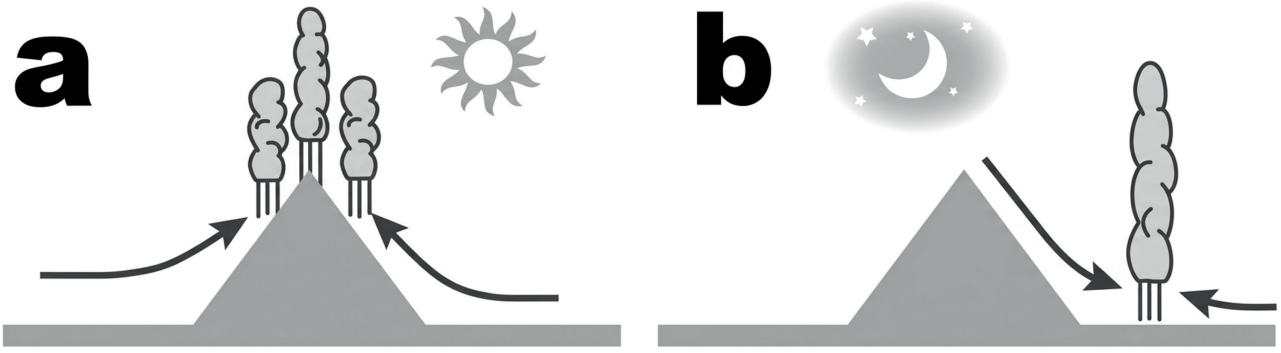

Fig. 5 Diurnal thermally induced initiation mechanisms that contribute to the formation of precipitating deep convection in the vicinity of mountains; (a) and (b) illustrate daytime and nighttime conditions, respectively, highlighting converging flows and forced ascent. Arrows indicate the direction of prevailing low-level airflows. Figure adapted from Houze (1993, his Fig. 12.24; 2012, his Fig. 3) with permission.

initiation corridors remain uncertain. Under strong low-level forcing or elevated thermodynamic anomalies, off-mountain nocturnal convection may evolve into large mesoscale convective systems that produce substantial nighttime precipitation across adjacent or even distant lowlands (e.g., Chu and Lin 2000; Damiani et al. 2008; Mulholland et al. 2020; Da Silva and Haerter 2023).

3.2 Airflow within valleys

Beyond slope flows, complex valley topography supports along- and cross-valley circulations that govern the mesoscale diurnal airflow (Markowski and Richardson 2010). These circulations are driven by ∇p arising from heating and cooling contrasts between higher elevations near the valley head and lower terrain at the valley mouth or adjacent plains (Fig. 4). Wagner et al. (2015) showed that valleys transport air from the surface to the free atmosphere three to four times more efficiently than flat terrain. Valley winds involve a larger air volume and typically higher velocities than slope winds and evolve on longer time scales (Serafin et al. 2018). When slope winds weaken or remain shallow, they are often overtaken by valley flows, although they still contribute to low-level cross-valley circulation (Figs. 3a, 4), which can at times exceed the along-valley component (e.g., Laiti et al. 2014).

The structure of valley airflow components and the associated air mass density changes depend strongly on valley geometry, including variations in width, depth, altitude, and orientation (e.g., Schmidli and Rotunno 2012). Blumen (1990) noted that differences in the air volume contained within valley sectors, or between a valley and an adjacent plain, strongly influence local flow behavior. This effect is quantified by the topographic amplification factor (TAF), a geometric measure of how efficiently a valley warms relative to a nearby plain based on the solar-exposed area and underlying air volume. Higher TAF values indicate more effective heating, which increases θ, lowers pressure up-valley, and strengthens the up-valley flow (e.g., De Wekker et al. 1998).

Daytime up-valley winds typically reach 1–8 m s^{-1} and often extend nearly to ridge height, with the deepening CBL focusing thermal hot spots and convergence near the valley head (e.g., Schmidli and Rotunno 2012; Bianco et al. 2011; Hagen et al. 2011). In deep, moist valleys, changes in $\partial\theta/\partial z$ and ∇p can persist all day, whereas in broader, drier valleys they develop within only a few hours, and particularly deep valleys may not generate flows strong enough to overcome CIN or capping inversions (e.g., Khodayar et al. 2013; Weckwerth et al. 2014). At night, the circulation reverses, becoming shallower and less intense (Serafin et al. 2018). Down-valley winds can develop a jet-like profile, with peak speeds near valley mouths up to 20 m s^{-1}, increasing low-level shear (e.g., Whiteman 2000). Although the cooler, stable air pool depresses the CBL and increases CIN (e.g., Kalthoff et al. 2011), CI can still occur where down-valley winds interact with circulations near the valley mouth or over the adjacent plain (Fig. 5b).

Temperature contrasts between the valley floor and opposing sidewalls generate weak cross-valley flows, producing a circulation that can favor stronger destabilization on one slope depending on time of day (De Wekker and Kossmann 2015). Combined with relatively strong slope winds, these contrasts create convergence and divergence zones over the valley floor, where ascending and descending motions compensate the paired slope flows (Fig. 4). In this context, valley channeling can superpose air masses of different origin and produce sharp gradients that are rarely resolved by coarse observations. Across studies (e.g., Laiti et al. 2014), valley-lake interactions can either suppress or enhance destabilization, depending on whether advection and subsidence dominate or whether moisture fluxes increase θ_e and CAPE locally. Feldmann et al. (2024) showed that in such cases large alpine lakes can amplify these thermodynamic anomalies and, together with channeling flows, enhance updraft strength in convective storms.

Under weak synoptic flow, the diurnal cycle of cross-valley winds often favors nocturnal CI in the valley center rather than along its margins, consistent with Fig. 5b. Although cold, stable air from surface cooling or precipitation-driven cold pools accumulates in the valley center, CI can still occur when these downslope-moving pools collide with residual upslope winds and enhance low-level convergence (e.g., Panosetti et al. 2016). Valley circulations also channel low-level flows, including warm and moist air from adjacent plains, through flanking slopes, tributary valleys, ridges, saddles, and gaps, where they interact with local thermals and background winds (e.g., Wang et al. 2016; Singh et al. 2022). In such cases, parcels may reach their LFC without needing to ascend to the mountain summit (e.g., Kottmeier et al. 2008; Weckwerth et al. 2011). An open question is when CI forms in the lee of mountains as valley flows from behind a ridge converge downstream, and whether modified low-level winds exert more control than ambient stratification (e.g., Barthlott et al. 2006; Hagen et al. 2011).

3.3 Airflow within basins

Basins are closed or semi-closed topographic depressions with wider floors than valleys and typically circular or oval shapes. Their circulation regimes resemble those of valleys, although classic up-valley winds are generally absent, and many valley-type circulations can still develop within basin atmosphere (Banta 1990). Basin geometry strongly influences thermally driven winds and vertical transport, and Barry (2008) identified three asymmetric basin-wind

regimes, of which shallow daytime upslope flow along the inner basin slopes is most relevant for CI (Fig. 5a). The strength of this upslope flow depends on slope steepness and the height of the basin floor relative to surrounding ridges. As in valleys, daytime upslope winds are compensated by subsidence and divergence in the basin center (e.g., Serafin and Zardi 2010). Because basin winds are often less affected by synoptic or mesoscale circulations, the primary limitation for daytime CI is the strong residual lid produced by nocturnal stable stratification, which likely varies across basin types and moisture regimes (e.g., Afrifa et al. 2025).

TAF enhances CBL growth in basins because the basin atmosphere warms more rapidly than the surrounding lowlands, while basin side slopes also supply substantial sensible heat fluxes that increase the diurnal temperature range (e.g., De Wekker et al. 1998). Resulting ∇T and ∇p drive winds into the basin atmosphere by late afternoon, allowing air to cross adjacent ridges with steeper $\partial\theta/\partial z > 0$ on their lee sides. These inflows may then collide with weakening inner-basin upslope flows, strengthening updrafts near the basin floor through added moisture and heat. De Wekker and Kossmann (2015) showed that the initial convergence zone forms on plain-side slopes and shifts toward basin slopes once the basin becomes warmer than the adjacent plains, although late-afternoon inflow surges from surrounding lowlands can abruptly shallow the CBL over nearby mountains and disrupt convergence around the basin.

3.4 Airflow over elevated plateaus

Elevated plateaus form a distinct type of thermally driven circulation, differing from basins primarily in that slope-wind forcing is shifted to the plateau margins rather than acting directly over the plateau interior. Thermally driven flows develop along the bordering hillsides and within the plain-to-plateau circulation, which directs low-level air toward the plateau with compensating return flow above the deep CBL. The height and horizontal extent of the plateau strongly determine the strength of this circulation, when the horizontal scale must exceed the typical CBL depth to generate meaningful mesoscale lifting (De Wekker and Kossmann 2015). Under strong solar heating and weak synoptic forcing, plateaus often develop a warm core (Chow et al. 2013). High-elevation plateaus exhibit less pronounced warm cores because vigorous convection enhances vertical heat loss, deepens the CBL, and strengthens horizontal ∇T across the plateau top (De Wekker et al. 1998).

Schmidli and Rotunno (2012) showed that plateau-induced warm cores elevate temperatures aloft over adjacent lowlands and valleys, intensifying along-valley ∇p and strengthening up-valley winds, often doubling their magnitude relative to valleys not bordered by a plateau. On a larger scale, the Spanish plume, a synoptic pattern associated with EMLs (Fig. 2; Ribeiro and Bosart 2018), has been viewed as analogous to such warm-core processes and predisposes western Europe to severe convection (e.g., Taszarek et al. 2020b). Schultz et al. (2025) argued that Spanish-plume EMLs need not originate over the Iberian Plateau and may instead develop over northern Africa or the Mediterranean Sea. Even when elevated terrain contributes, diurnal heating produces transient warm anomalies rather than a continuous plume. These anomalies do not always coincide with favored CI, with strong sensitivity to the low-level flow, and the controlling mechanisms remain poorly quantified.

Plateau circulations are often weak, so they may transport limited low-level moisture onto the plateau with reduced CAPE. They are also easily overwhelmed by synoptic flows, limiting the influence of TAF and reducing diurnal temperature amplitudes. On the other hand, morning instability and cold-air drainage can support large-scale plateau updrafts, and persistent afternoon convergence zones along the plateau edge may promote CI, further enhanced by peripheral upslope winds. Laboratory experiments by Goldshmid et al. (2018) showed that upslope thermals may detach from the surface under certain slope and plateau geometries, reducing their ability to feed the plateau-core updraft and the associated convergence, so additional horizontal entrainment is required to sustain CI-relevant lifting. In contrast, escarpment-like slopes maintain attached upslope flow that more effectively reinforces the plateau core. When turbulent convection over the plateau weakens, opposing density currents may collide and stabilize the environment or provide mechanical lifting that can bring moist low-level air to saturation. In this context, more generally, sustained low-level updrafts preceding CI may need to exceed a critical horizontal scale (approximately 3–5 km) to withstand midlevel dry-air entrainment, as suggested by Marquis et al. (2021).

Furthermore, findings from several idealized studies (e.g., Kirshbaum 2013; Hassanzadeh et al. 2016; Panosetti et al. 2016; Imamovic et al. 2019) suggest that both the volume and orientation of plateau-like terrain relative to ambient winds influence the preferred location of CI and associated precipitation patterns, although these sensitivities may not generalize across mountain heterogeneity and varying synoptic forcing. Imamovic et al. (2019) showed that convective precipitation scales linearly with mountain volume and increases for flows parallel to the major axis of the mountain, while stronger background winds tend to shift CI maxima downwind and reduce precipitation efficiency. Hassanzadeh et al. (2016) likewise found that precipitation intensity increases with mountain height until the terrain becomes tall enough for synoptic winds to deflect or split the flow around it.

3.5 Mountain-plain transition circulations

Although slope, valley, basin, and plateau winds can extend over broad areas, they rarely match the larger-scale thermally driven air exchange that develops between a substantial mountain massif and the surrounding lowlands (Fig. 4). Such circulations can reach the upper end of the mesoscale and may exhibit diurnally oscillating behavior (Barry 2008). A prominent example is the Alpine Pump, a thermally induced circulation in which low-level air is drawn from adjacent plains toward a thermal low over the Alps, with substantial effects on directional wind shear and storm organization near the range (e.g., Trefalt et al. 2018). Graf et al. (2016) found that this circulation occurs on roughly 62 days per year and influences lowland airflow up to 100 km away, with simulated up-mountain inflow depths reaching about 1.5 km. However, key uncertainties remain in how plain-to-mountain and valley circulations determine the source regions and thermodynamic properties of the inflow air that ultimately feeds cloud-base updrafts.

The plain-to-mountain circulation (and its nocturnal reverse) extends over the height of the mountain ridge and overlies smaller slope and valley flows but is generally too weak to dominate them (Fig. 3a). It acts mainly in the upper part of the mountain boundary layer. During the day, negative ∇p toward the mountains generates up-mountain winds from adjacent plains, with typical speeds up to about 2 m s^{-1} and a broad compensating return flow aloft. Although easily suppressed by stronger ambient winds (e.g., Lareau et al. 2024), these flows can still transport key thermodynamic ingredients over long distances or shift drylines that support deep CI downwind of higher mountains (e.g., Bergmaier and Geerts 2015). The nocturnal phase is shallower, weaker, and reversed. Plain-mountain circulations also adjust more slowly to ∇T and ∇p than other thermally driven flows, producing time-shifted transition periods (Fig. 3b).

Persistent up-mountain transport causes the CBL to bulge upward, forming a thermal hot spot that can encompass an entire range. Yet, the presence of a range-scale hot spot does not necessarily imply uniformly favorable thermodynamic conditions across all internal ranges and basins, because the resulting vertical profiles depend on tropospheric depth and because temperature and moisture generally decrease with elevation. Nevertheless, observational studies (e.g., Weckwerth et al. 2011; Lock and Houston 2015; Lombardo and Bitting 2024) showed that CI occurs far more frequently over mountain ranges than over adjacent lowlands, with CI densities over the mountains about twice those in valleys and plains. Mountain volume and the interaction of thermal and ambient winds govern where CI subsequently expands (e.g., Levizzani et al. 2010; Hassanzadeh et al. 2016; Imamovic et al. 2017, 2019).

The analysis of prestorm environments in the Western Carpathians provides an illustrative example of how these controls shape the buoyancy field under contrasting wind regimes (Fig. 6). In a weak-wind, weak-forcing regime associated with slow-moving supercells forming closer to the mountains (Fig. 6a), CAPE is comparatively uniform across ranges, valleys, and basins, with the dominant gradient primarily controlled by elevation and decreasing toward higher terrain. By contrast, under stronger synoptic forcing associated with faster-moving supercells forming predominantly farther from the major ranges (Fig. 6b), CAPE exhibits a markedly different pattern. It is substantially reduced over windward slopes during prevailing southwesterly to westerly mid- to upper-level flow and can be suppressed even over lower mountains which showed elevated buoyancy in a weaker regime. At the same time, larger air-mass contrasts emerge across the region, such that well-ventilated mountain areas embedded within cooler, drier air exhibit markedly lower CAPE, whereas leeside mountains that remain within warmer and moister air can retain appreciable buoyancy and thermally driven low-level winds that are maintained despite stronger synoptic flow. Under these strong-flow conditions, terrain-flow interaction can also generate leeside convergence zones and displace thermally favored initiation regions downwind (e.g., Kirshbaum 2017; Reif and Bluestein 2018).

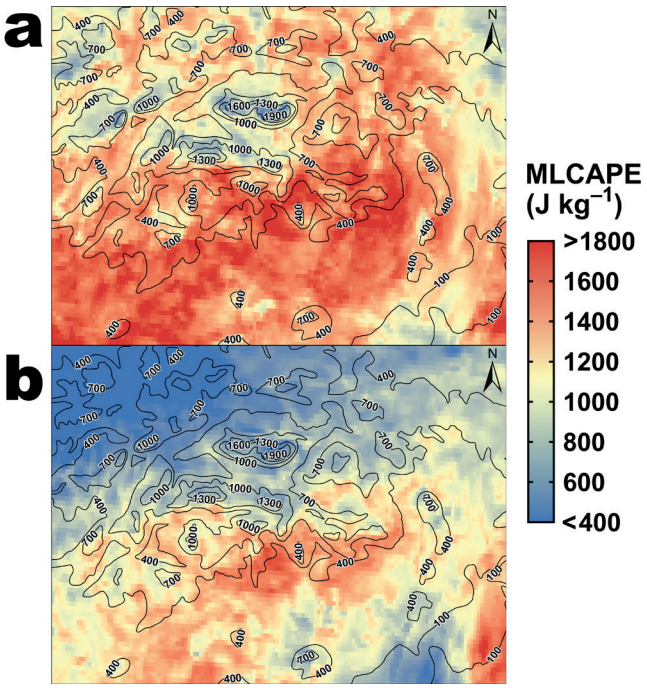

Fig. 6 Spatial distribution of median mixed-layer CAPE (0–500 m AGL parcel) from COSMO simulations over the Western Carpathians prior to supercell initiation. Panels show (a) slow-moving supercells in a weak-wind regime and (b) fast-moving supercells in a strong-wind regime, with predominant southwesterly-westerly mid- to upper-tropospheric flow. Smoothed elevation contours are shown every 300 m above mean sea level and topographic features with boundary lengths < 23 km are excluded.

Plain-to-mountain winds opposing the flow aloft can further modify leeside vertical shear and hodograph curvature, thereby influencing supercell initiation (e.g., Soderholm et al. 2014; Scheffknecht et al. 2017; Mulholland et al. 2019). Indeed, Kvak et al. (2023) found that 68% of the studied mesocyclones emerged over the leeward slopes of the Carpathians, although the first CI signatures may appear farther upstream. Yet larger samples and regime-based stratification are needed to separate robust signals from anomalous events. Moreover, although recent work has substantially expanded understanding of terrain effects on supercell environments (e.g., Purpura et al. 2023; Feldmann et al. 2024; McKeown et al. 2024; Riggin et al. 2025), it remains unclear under what combinations of terrain-forced convergence, buoyancy, and storm-relative flow supercells can form and persist when deep-layer shear is weak (e.g., Tang et al. 2016).

4. Mechanically forced orographic flow perturbations

Mechanically forced ascent occurs when a sufficiently strong large-scale flow impinges on terrain and undergoes terrain-flow interaction within the mountain environment (e.g., Kirshbaum et al. 2007; Barrett et al. 2015; Lareau et al. 2024). It is most prominent under moderate to strong ambient flow, when lift patterns are controlled mainly by flow direction, stability, and terrain geometry, and CI occurs where the resulting ascent is deep enough to lift moist air to its LFC while CIN is weak enough to be overcome by the available lift (e.g., Marquis et al. 2023). Terrain alters both the vertical and horizontal wind components, which can support CI by lifting parcels through forced ascent, by generating low-level convergence zones, and by producing upward acceleration in ducted orographic waves near mountains (e.g., Markowski and Richardson 2010; Nelson et al. 2021; Nicolas and Boos 2022) that locally modulate the vertical depth of moisture and parcel buoyancy.

Nonetheless, mechanically forced ascent alone is not sufficient for CI. Its effectiveness depends on whether sufficiently moist, conditionally unstable air is present (or becomes locally enhanced) and on how terrain-induced subsidence and mixing in adjacent lee regions modify moisture and CAPE, potentially strengthening CIN and suppressing CI (e.g., Marquis et al. 2023). Accordingly, CI tends to occur where terrain-modified convergence and moisture transport maintain or increase low-level moisture and reduce inhibition enough to permit ascent to the LFC. Resulting deformation of the wind field strongly affects low-level flow and can modify the magnitude of vertical wind shear (e.g., Mulholland et al. 2019). Because shear helps govern storm organization and longevity once CI occurs, terrain-driven shear modulation can either favor or inhibit both CI and subsequent storm organization in the vicinity of mountains (e.g., Houze et al. 1993; Markowski and Dotzek 2011; Mulholland et al. 2020; Feldmann et al. 2021; Da Silva and Haerter 2023).

Key factors that influence mechanically forced ascent and determine whether air ascends a mountain or becomes blocked include the upstream stability, the strength of the impinging flow, and the spatial extent of the barrier (e.g., Whiteman 2000; Reeves and Lin 2007; Miglietta and Rotunno 2014; Degiacomi et al. 2025). The terrain shape relative to the flow, its vertical and horizontal scales, surface roughness, and the arrangement of ridges and valleys further modulate the flow response and thereby the spatial distribution of low-level moisture and instability in the vicinity of mountains (Fig. 6; e.g., Roe 2005; Imamovic et al. 2019; Ammon et al. 2025). Less stable upstream flow, sufficiently strong incoming winds, and a narrow barrier favor ascent over the terrain and flow crossing the ridge, with CI often developing along windward slopes (e.g., Chen and Lin 2005). In contrast, more stable air with $\partial\theta_e/\partial z > 0$, weaker flow, and a broad barrier promotes partial or complete blocking. The flow then detours the obstacle, and CI is more likely upstream, downstream, or around the terrain rather than directly over it (e.g., Frame and Markowski 2006).

Both vertically and horizontally, terrain-modified wind effects are strongest near large mountains that interact with upper-level flow or lie within dynamically active regions (e.g., Barry 2008). Elevated terrain can slow synoptic low-level flow through increased surface friction, yet compression and channeling of the impinging airstream may locally accelerate mesoscale currents (e.g., Houze 2012; Tang et al. 2016). Strong background flow can also advect surface-based buoyancy anomalies, such as warm thermal wakes, into the lee, where they interact with mechanically induced CI (e.g., Bougeault et al. 2001; Kirshbaum and Wang 2014). These modified wind and buoyancy patterns are consistent with a foreland maximum in the overlap of lift, moisture, and weak inhibition, which can also favor environments supportive of hailstorms (e.g., Punge and Kunz 2016; Battaglioli et al. 2023). Although mountain-flow regime concepts are harder to apply in conditionally unstable environments or in elevated convection (e.g., Kirshbaum et al. 2018), the evolution of moist low-level air remains critical for CI (e.g., Weckwerth et al. 2014; Wang et al. 2016).

4.1 Vertical deformation of the background wind field

Orographic flow modification occurs regardless of how susceptible the low-level air is to blocking, since commonly used blocking diagnostics describe only whether near-surface flow tends to ascend over or detour around a barrier (e.g., Hagen et al. 2011; Kirshbaum et al. 2018). Even when the low-level flow would

ordinarily ascend the terrain, any vertically stacked air column that is not absolutely unstable experiences at least some degree of blocking or deflection as it encounters the mountain (Blumen 1990; Kirshbaum and Wang 2014; Kirshbaum 2017). Airflow approaching complex terrain is forced to compress and converge near the surface and within the lower troposphere. Density and cross-barrier velocity of the impinging air, together with terrain characteristics such as slope angle and horizontal extent, control the intensity of vertical deformation (Hilel Goldshmid et al. 2018). These momentum perturbations can extend vertically through much of the troposphere, and even hills only a few hundred meters high can disrupt an otherwise balanced wind field (e.g., Kirshbaum and Schultz 2018).

Moist, conditionally unstable air that is not blocked or diverted is mechanically forced to rise and cross part or all of the terrain (e.g., Miglietta and Rotunno 2014). Static destabilization associated with thermal circulations, together with reduced upstream blocking, further promotes terrain-forced ascent and lowers CIN within the windward CBL by deepening the mixed layer and increasing near-surface θ_e (e.g., Chu and Lin 2000; Riggin et al. 2025). Fig. 7a illustrates a CI mechanism in which a positive vertical-velocity anomaly and a convergence zone develop over windward slopes, allowing even modest ambient flow to provide sufficiently deep mechanically forced lift to raise moist conditionally unstable air to its LFC (Lock and Houston 2014). Windward ascent is a common mechanism for CI and convective precipitation enhancement (e.g., Hagen et al. 2011; Kirshbaum et al. 2016; Bačová Mitková et al. 2018). Even under stronger stability, a potentially unstable layer within a stratiform precipitating system may still be lifted to its LFC, producing embedded convection when sufficient midlevel moisture and lapse rates support elevated CAPE above a stable near-surface layer (e.g., Davolio et al. 2016; Friedrich et al. 2016; Kašpar et al. 2021).

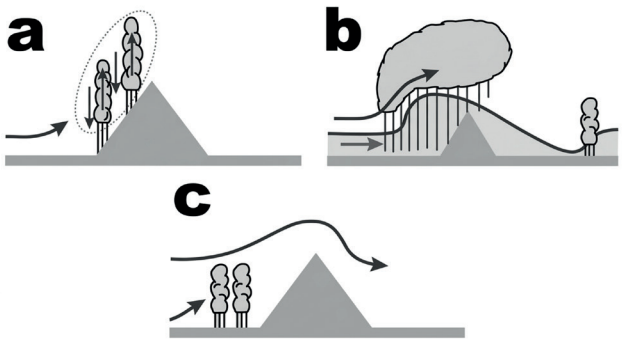

Fig. 7 Mechanically induced initiation mechanisms that contribute to the formation of precipitating deep convection in the vicinity of mountains. (a) Terrain-forced ascent along windward slopes, (b) downslope-propagating outflows from stratiform or convective precipitation, and (c) partially or fully blocked low-level flow. Arrows indicate the direction of prevailing airflows. Figure adapted from Houze (1993, his Fig. 12.24; 2012, his Fig. 3) with permission.

Once thunderstorms develop over mountains, or when stratiform precipitation is present, cold pools and outflows can propagate rapidly downstream and downslope, supporting distant CI (Fig. 7b) along convergence zones, thermal contrasts, or hydraulic-jump-like transitions, where CAPE is preserved by moisture pooling on the warm side of the boundary (e.g., Reeves and Lin 2007; Kirshbaum and Schultz 2018; Schneider et al. 2018; Nicolas and Boos 2022). In conditionally unstable environments, strong ascent along these jumps can initiate new convection or reinvigorate existing storms (e.g., Chu and Lin 2000; Frame and Markowski 2006; Smith et al. 2015). Under weaker background winds, outflows can interact with opposing upslope flow and regenerate CI upstream through new cell development (e.g., Chen and Lin 2005; Miglietta and Rotunno 2014; Panziera et al. 2015).

Apparent outflow-like signatures (Fig. 7b) in the lee of mountain ranges can also arise from non-precipitating processes, including downslope-wind descent and turbulent mixing that substantially dry the boundary layer and reduce surface-based CAPE during synoptic-scale cross-barrier flow (e.g., Kaspar et al. 2009). This mountain-induced mixing often does not suppress CI everywhere. Instead, it displaces the most favorable CI corridor to the edge of the lee-modified air mass, where a dryline-like moisture boundary and sharp instability gradient form along the foreland, focusing low-level convergence while preserving buoyancy on the moist side (e.g., Bergmaier and Geerts 2015). Downwind CI can therefore occur well away from the mountains when a downslope surge undercuts or abuts a moist boundary-layer reservoir, yielding a narrow corridor where CIN is locally reduced despite widespread drying nearby. Such complex interactions among local terrain-forced lift, leeside mixing, gust-front lifting, and free-tropospheric entrainment in sustaining convection after CI are not easily quantified even in high-resolution models, complicating CI diagnosis and forecasting (e.g., Kaltenboeck and Steinheimer 2015; Marquis et al. 2023).

Fig. 7c illustrates a CI mechanism in which the mountain height greatly exceeds the LFC and the upstream flow is partially or fully blocked and stable. In such cases, pulsing CI may develop where the airstream is forced to bend upward, and the conditionally unstable layer first reaches its LFC provided that sufficient moisture is retained to sustain CAPE and CIN is locally reduced by the convergence-driven ascent (Houze 1993). When blocking extends through a deep layer, wind speed can decrease sharply in front of the mountain, and the resulting convergence may produce a hydraulic-jump-like transition with enhanced upward motion (Řezáčová et al. 2007). This feature can shift CI well away from the barrier on the upstream side (e.g., Davolio et al. 2016). In upstream-blocking regimes, deep convective clouds are often lower because the upper troposphere is

more stable, the available CAPE is limited, and strong vertical shear tilts and weakens updrafts.

Mechanically forced ascent on the lee side can generate lee waves that initiate convective clouds downstream of hills or modest mountains when sufficient moisture and CAPE are present and CIN can be breached (e.g., Kirshbaum et al. 2007). Fig. 8a shows a CI mechanism in which lee waves arise as stable flow ($\partial\theta/\partial z > 0$) passes over a small mountain, producing oscillating pressure, wind, and buoyancy anomalies (e.g., Serafin et al. 2018). Leeside lifting and flow acceleration create a pressure trough that draws air inward and forms a convergence zone where moisture can pool and enhance parcel buoyancy (e.g., Kirshbaum et al. 2016). For strong-flow regimes, it is not fully resolved how terrain geometry and stratification control the evolution and persistence of leeside convergence and its effectiveness for CI. If the leeside terrain slopes upward or environmental conditions favor persistent ascent, these waves can initiate precipitating convective clouds that are advected downwind as narrow rainbands aligned with the flow (e.g., Barrett et al. 2015; Kirshbaum and Schultz 2018a; Degiacomi et al. 2025). Turbulence, separation eddies, and wakes near the surface or within the mountain CBL may further enhance ascent, especially in complex or forested terrain where surface roughness strengthens small-scale convergence and intermittently lifts parcels through the residual inhibition (e.g., Whiteman 2000; De Wekker et al. 2018).

Another CI mechanism (Fig. 8b) involves vertically propagating mountain waves that develop over higher and steeper terrain and tilt upstream, producing persistent wave-induced ascent and quasi-stationary CI near prominent crests (e.g., Chu and Lin 2000). These waves, sustained in stable environments, may amplify above the crest and interact with moist low-level inflow, yielding elevated CI downstream of the mountain (e.g., Reif and Bluestein 2018; Feng et al. 2022). Nevertheless, it is not yet clear how upstream surface fluxes precondition the inflow humidity and static stability that modulate mechanically forced CI through their control on CAPE and CIN in the inflow layer. Figs. 9i, j show simulations of Mulholland et al. (2019) when higher terrain generates stronger and deeper waves, evident from bent-back isentropes and enhanced upward motion. In these cases, standing waves with vertical velocities of 1–4 m s^{-1} formed near the ridgetop, while the mixed-layer LFC was lower over the crest. This combination of larger wave amplitude, stronger ascent, and reduced LFC height produced earlier CI by weakening the effective inhibition. By contrast, lower terrain yielded weak or absent mountain waves (Figs. 9f, g) and higher ridgetop LFCs, delaying CI.

4.2 Horizontal deformation of the background wind field

Orographically forced horizontal flow modifications are important for CI in complex terrain because they create convergence zones, shift initiation maxima away from peaks (e.g., Wang et al. 2016), transport heat and moisture, and displace unstable layers (e.g., Ribeiro and Bosart 2018). As with vertically forced motions, they occur regardless of blocking, although when low-level flow cannot surmount the barrier, a larger fraction is diverted laterally (Blumen 1990). Air more readily detours around tall, narrow, or isolated peaks than around broad or elongated ranges oriented perpendicular to the inflow. Surface characteristics, ridge orientation, and curvature strongly influence wind direction and speed along the flanks (e.g., Reif and Bluestein 2018; Ammon et al. 2025), with parallel or convex terrain promoting efficient lateral deflection and sharpening low-level moisture gradients between deflected inflow and adjacent mixed or subsident air (Whiteman 2000). Depending on the terrain shape, the flow may accelerate along one side or separate around the lateral edges (Houze 1993), and because these modifications act within the moist low-level layer, they can efficiently promote CI (Kirshbaum and Wang 2014).

When upstream blocking or stagnation occurs, and depending on the mountain geometry and the lower terrain downstream, the flow often diverts around the lower flanks rather than over the higher summits (e.g., Hagen et al. 2011). Under weaker

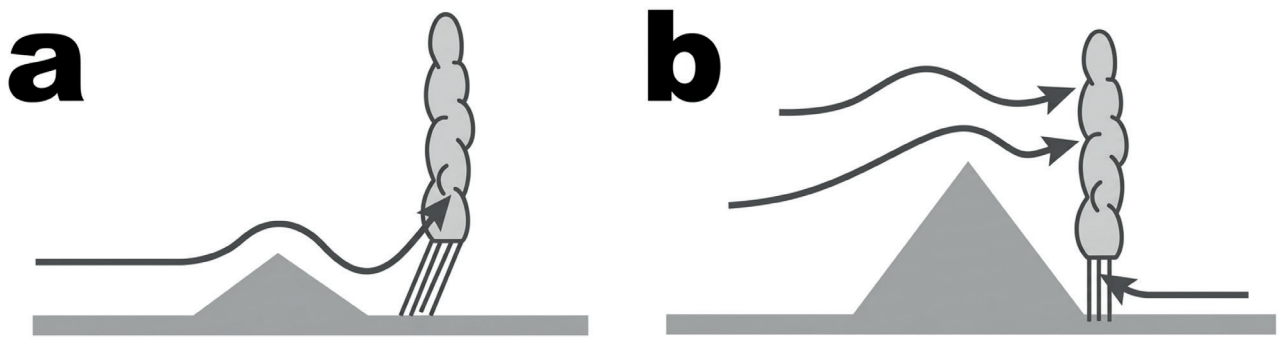

Fig. 8 As in Fig. 7, but showing: (a) downstream lee-wave convection initiated by ascent in the lee-wave crests downstream of hills or low mountains, and (b) upstream-tilted vertically propagating mountain waves over higher terrain. Figure adapted from Houze (1993, his Fig. 12.24; 2012, his Fig. 3) with permission.

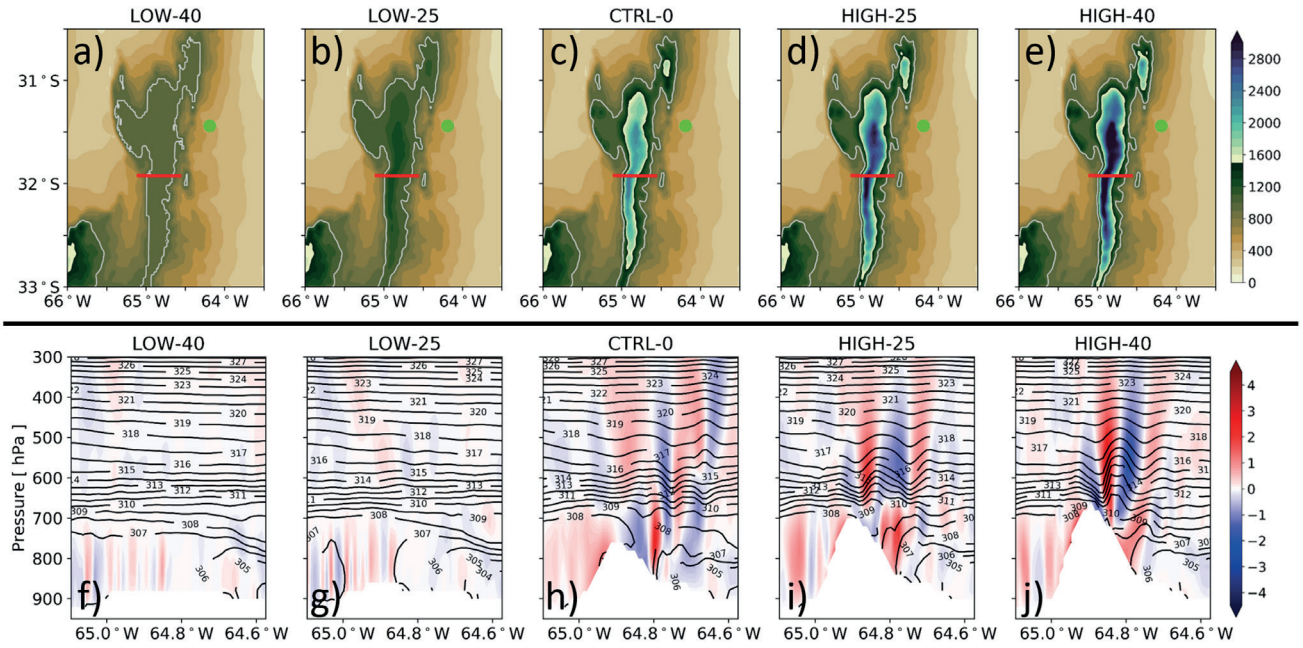

Fig. 9 Orographic model experiments illustrating vertically propagating mountain waves over the Sierras de Córdoba, Argentina, on 29 November 2017. Panels (a–e) display plan-view terrain height (shaded; m), the 1000-m elevation contour (gray), the location of Córdoba (lime dot), and the west-east cross-section transects (red lines) corresponding to the lower panels (f–j). In panel (h), CTRL-0 provides the baseline terrain configuration, whereas panels (f) LOW-40, (g) LOW-25, (i) HIGH-25, and (j) HIGH-40 depict terrain reductions or increases of 40%, 25%, 25%, and 40%, respectively. The vertical sections (f–j) show vertical velocity (shaded; m s^{-1}) and potential temperature (black contours at 1-K intervals) at 1500 UTC 29 November 2017. Figure reproduced from Mulholland et al. (2019, their Fig. 2) with permission.

winds, the separated flow commonly reassembles in a confluence zone with accumulated moisture and reduced CIN. Because these confluence zones shift between events, composite analyses may obscure the true placement and timing of the peak ascent (e.g., Bougeault et al. 2001; Schneider et al. 2018). Fig. 10a presents a CI mechanism in which the confluence of deflected and ambient flows generates ascent in the lee, with further upward acceleration possibly enhanced through interaction with vertically displaced flows (e.g., Kirshbaum and Schultz 2018a). CI may also develop under stronger background winds along the path of the diverted flow on extended mountain flanks, where stronger low-level winds allow the deflected branch to merge with the environmental flow and form a flanking convergence zone along one or both sides of the barrier (Banta 1990).

Diverted airflow may form an elevated barrier jet along windward slopes, blowing parallel to the mountain and strongest near the foothills (Chow et al. 2013). Although barrier jets are often associated with winter cold-air surges, they also occur in summer and can contribute to CI (e.g., Davolio et al. 2016; Nicolas and Boos 2022; Singh et al. 2022). Their characteristics depend on synoptic forcing, regional climate, and mountain geometry, which together determine the prevailing flow regime (Houze 2012; Ribeiro and Bosart 2018). Such low-level jets transport moisture over long distances, favor high-CAPE environments (e.g., Chu and Lin 2000; Feng et al. 2022), and, when acting as barrier jets, can exceed 15 m s^{-1} up to 500 m AGL (Whiteman 2000), thereby also increasing low-level shear (Reif and Bluestein 2018). However, strong shear within these jets can hinder CI by

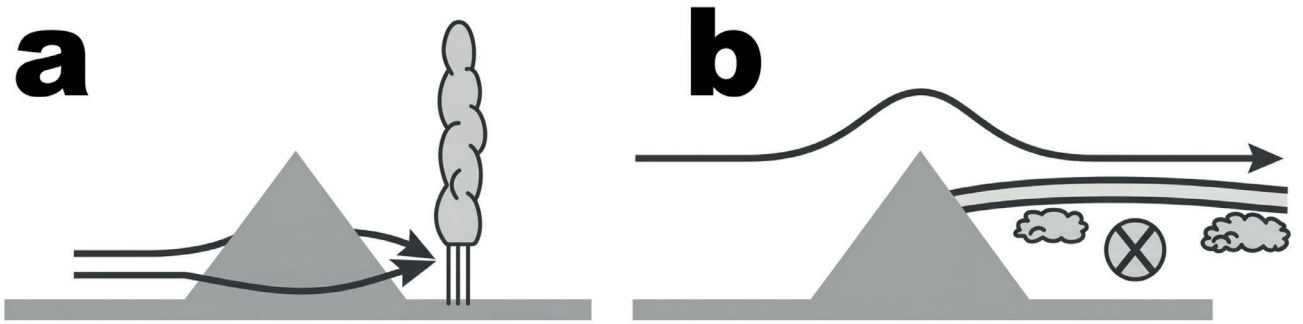

Fig. 10 As in Fig. 7, but showing: (a) the deflection of low-level flows around the terrain and their confluence in the lee, and (b) an elevated mixed layer is horizontally advected off the horizontal advection of an elevated mixed layer from the mountains over adjacent plains, creating a capped but potentially unstable environment. Figure adapted from Houze (1993, his Fig. 12.24; 2012, his Fig. 3) with permission.

disrupting developing updrafts (Markowski and Richardson 2010).

Within valleys, gorges, gaps, and passes, airflow is laterally and vertically constricted and becomes channeled, enhancing low-level moisture transport (e.g., Wulfmeyer et al. 2011; Tang et al. 2016; Singh et al. 2022). The strength and depth of these gap flows depend on upstream-downstream differences in $\partial\theta/\partial z$ and on hydrostatically driven ∇p through the narrowed terrain (e.g., Schmidli and Rotunno 2012; Chow et al. 2013). Downstream, the flow commonly shows a wind-speed maximum, enhanced turbulent mixing beneath a stagnant cap, and sometimes a hydraulic-jump-like rebound (Markowski and Richardson 2010). Because the gap entrance is typically more stable, CI there is uncommon. Instead, outflowing air more often encounters more favorable conditions just downstream, where CIN is minimized and CAPE, though reduced, can still support CI along the exit flanks (e.g., Markowski and Dotzek 2011). When the outflow aligns with the along-gap axis, it may also enhance storm dynamics (Riggin et al. 2025), raising the question of how different terrain features interact with low-level winds and storm motion.

In another example of terrain-modified low-level flow, Wang et al. (2016) showed that CI along the Dabie Mountains ridge results from the interaction of thermally driven upslope winds, mechanically deflected around-peak flow, and valley-channeled upslope currents (Fig. 11). This configuration aligned convergence zones along the ridge, shifted them slightly downwind, and produced the strongest lifting

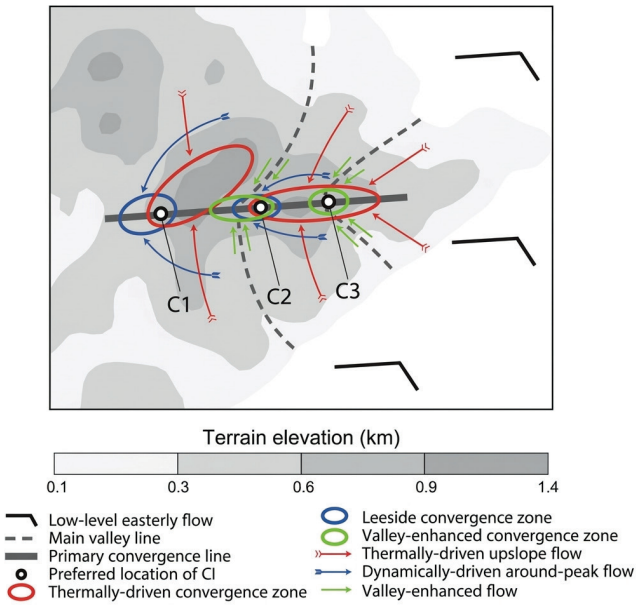

Fig. 11 Low-level convergence zones over the Dabie Mountains ridge, China, on 10 June 2010. Wind barbs depict the ambient low-level flow, while colored arrows show the main terrain-modified currents. The bold gray line marks the primary convergence zone above the ridge where these flows interact. White-filled black circles (C1, C2, C3) denote the three major deep convective cells initiated before 0600 UTC. Figure reproduced from Wang et al. (2016, their Fig. 13) with permission.

and earliest CI where two or more convergence mechanisms overlapped and where low-level moisture was deepest, allowing parcels to access buoyancy with minimal inhibition. Soderholm et al. (2014) similarly found that quasi-stationary storms are favored when low-level winds run parallel to a ridge, allowing outflows to propagate downwind without disrupting the upslope inflow that maintains elevated convergence, whereas cross-ridge flow suppresses repeated CI. The behavior of these outflows depends on terrain steepness and rain-induced momentum, as steeper mountains slow their lateral spread and modulate their interaction with elevated convergence zones (Imamovic et al. 2019).

The last orographically influenced CI process, illustrated in Fig. 10b, is more indirect because it does not generate ascent itself but instead involves horizontal displacement of a surface-based capping inversion from mountains toward adjacent lowlands. EMLs that form over mountains may be partially or fully advected off the terrain by terrain-modified ambient winds (Fig. 2). Such environments are common east of the Rockies and Andes (e.g., Ribeiro and Bosart 2018) and north-northwest of the Meseta Central (e.g., Schultz et al. 2025) and do not entirely prevent CI (e.g., Bergmaier and Geerts 2015; Taszarek et al. 2020b; Nelson et al. 2021). When sufficient mesoscale lift develops later in the day (e.g., Fig. 7b; Doswell 1987), the cap can be breached, and parcels can reach their LFCs. By modifying the thermodynamic profile and delaying early CAPE release, these elevated layers allow potential instability to accumulate far downstream from the EML source, making mountains a significant, albeit indirect, contributor to intense severe convection once lifting finally overcomes CIN (e.g., Doswell and Bosart 2001; Kaspar et al. 2009; Kunz et al. 2018).

5. Summary and perspectives

This review brings together current understanding of how orography influences convective storm initiation within a mesoscale framework. Houze (2012) emphasized that topography acts as a passive boundary condition in precipitation processes and does not itself provide the essential ingredients for convective storm formation. In many cases, the large-scale environment would still support thunderstorms over flat terrain, although their timing and location would differ without orographic effects. Orography modifies all three ingredients required for CI, namely moisture, instability, and lift, by redistributing heat and moisture, reorganizing low-level flow, and providing localized ascent (Doswell et al. 1996). These modifications arise through thermally driven circulations that are most prominent under weak background flow and strong diurnal heating, and through mechanically forced flow perturbations that become

more influential under moderate to strong ambient flow. Together, these terrain-atmosphere interactions create mesoscale convergence and ascent and can precondition the thermodynamic environment so that parcels reach the level of free convection, above which buoyant acceleration proceeds largely independent of the underlying terrain as cumulonimbus clouds develop.

Thermally driven circulations emerging from diurnal differential heating across slopes, valleys, basins, plateaus, and adjacent plains organize the mountain boundary layer and strongly influence CI. Upslope flows, the primary low-level response to daytime heating, create greater instability and convergence along sunlit slopes and ridges where CI often begins. Valley geometry modulates up-valley transport, boundary-layer growth, and erosion of convective inhibition, while basins, plateaus, and larger massifs support broader plain-to-mountain inflows that transport moist, unstable air and focus ascent along terrain edges. Upslope and up-valley transport can deepen the boundary layer and create convective hot spots. Under stronger background flow, terrain-flow interaction can displace these hot spots downwind and can also produce leeside convergence zones. At night, radiative cooling stabilizes higher terrain and nearby valleys, but downslope and down-valley flows can still support CI where they encounter moist air. Observations show that CI occurs more frequently over mountains than adjacent lowlands, with a late-morning to early-afternoon maximum that reflects the dominant role of diurnal thermal circulations in modulating buoyancy, moisture, and low-level convergence.

Mechanically based terrain effects profoundly modify low-level flow and redistribute thermodynamic properties through forced ascent, leeside subsidence and mixing, deflection, channeling, and splitting, and these adjustments often control when and where CI occurs. Whether air ascends a barrier or detours around it depends on static stability, wind speed and direction, and terrain geometry, which can shift CI to windward slopes, leeside convergence zones, flanks, or upstream regions. Thermally driven upslope winds, mechanically deflected cross-barrier flows, and valley-channeled currents frequently converge to form persistent lifting corridors, while cold-pool outflows, hydraulic-jump-like transitions, and dryline-like moisture boundaries can regenerate CI, shift it downstream, or locally suppress it. Mountain waves provide additional elevated ascent that can anchor quasi-stationary CI over and downstream of high terrain, and terrain-modified vertical shear further shapes storm organization. Mountains also influence CI indirectly by producing elevated mixed layers that are advected over adjacent plains, delaying convection while allowing substantial convective available potential energy accumulation until mesoscale ascent finally erodes the cap.

With increasing terrain height, the relative importance of mechanically forced processes generally increases during strong-flow situations, because windward ascent, blocking and deflection, lee convergence, and mountain-wave responses become more pronounced. In low mountain ranges and hilly terrain, thermally driven circulations often provide the dominant mesoscale mechanism during weak-flow warm-season conditions. In medium to high mountain ranges, thermally driven circulations still frequently precondition the boundary layer through moisture transport and erosion of convective inhibition, but mechanically forced lift and lee convergence more often determine where and when initiation occurs during periods of synoptic-scale forcing.

5.1 Open questions and research priorities

A central research need is to move from documenting where CI occurs in mountains to explaining why it occurs preferentially in certain terrain features and flow regimes, by tracing how terrain-driven processes modify the CI ingredients and interact across multiple scales (e.g., Imamovic et al. 2019; Rotach et al. 2022). For thermally driven regimes, key unknowns include how valley and plain-to-mountain circulations set the source regions and thermodynamic properties of rising parcels, and how boundary-layer heterogeneity controls effective convective inhibition and the width and depth of cloud-base updrafts as thermals transition through the capping layer into the free troposphere (e.g., Marquis et al. 2021; Nelson et al. 2022). For mechanically forced regimes, major gaps persist in quantifying transient and nonlinear processes such as the evolution of leeside convergence, cloud-diabatic feedbacks on mountain waves and blocking, and the role of upstream surface fluxes in preconditioning stability and humidity (e.g., Kirshbaum et al. 2018; Nicolas and Boos 2022). Across both regimes, the challenge is not only the mean forcing but also the organization of lift in space and time, including how terrain channeling can superpose air masses of different origin and create sharp gradients in moisture, convective inhibition, and low-level shear that are rarely resolved by coarse observations or compositing approaches (e.g., Markowski and Dotzek 2011; Lareau et al. 2024).

Progress on these questions will require coordinated strategies that link CI mechanisms to CI outcomes using complementary observations and modeling. Priorities include (i) dense, three-dimensional measurements of near-cloud thermodynamics, convergence, and turbulence across valleys, slopes, ridges, and adjacent plains, with scanning strategies designed to test explicit hypotheses about CI (e.g., Serafin et al. 2018; Marquis et al. 2023); (ii) systematic numerical experimentation spanning convection-permitting to large-eddy simulation scales to isolate sensitivities to terrain geometry, land-surface heterogeneity,

and background flow, while addressing marginally resolved terrain forcing in simulations of orographic CI (e.g., De Wekker and Kossmann 2015; Panosetti et al. 2016); and (iii) analysis frameworks that distinguish robust regimes from anomalies through larger samples, more sophisticated statistical tools, and alternative stratification by wind speed, shear, instability, and flow direction in different terrain settings (e.g., Katona et al. 2016; Kvak et al. 2023).

Supercells and other organized storms provide a useful test for these efforts because they amplify small terrain-driven changes in low-level flow and hodograph structure, yet are difficult to confirm observationally in complex terrain (e.g., Scheffknecht et al. 2017; Da Silva and Haerter 2023). Research priorities therefore include identifying when thermally driven circulations meaningfully enhance low-level shear and storm-relative inflow, how leeside convergence corridors modulate storm initiation likelihood, and under what conditions terrain-forced lifting and heterogeneity can compensate for weak deep-layer shear to support persistent rotating updrafts (e.g., Fischer et al. 2025).

In mountainous regions where convective storms occur at least seasonally, orographically induced flows create distinctive environments in which storm activity differs in several important ways from that over lower elevations. Of greatest societal relevance are a higher frequency of storm initiation, an increased likelihood of convection-related severe weather, and greater uncertainty in forecasts of both storm occurrence and intensity (e.g., Barrett et al. 2015; Kühne et al. 2025). Despite substantial progress, many processes remain difficult to quantify, limiting operational forecast accuracy and the ability to anticipate societal impacts (Brooks et al. 2019). Quantitative statistics comparing the prevalence of specific CI mechanisms across mountain settings and flow regimes within a given region also remain limited, highlighting a need for expanded observations and targeted modeling. Readers are encouraged to consult the references cited herein for more detailed discussion, as a comprehensive treatment of all issues lies beyond the scope of this condensed review, but the priorities outlined above provide a path toward improved understanding and predictability.

Acknowledgments

We thank Miloslav Müller and Petr Zacharov for their comments and encouragement and Miroslav Truben for assistance with the figure illustrating idealized thermally driven circulations over a mountain. We also thank the authors who granted permission to reproduce figures from their publications. We appreciate the constructive feedback from two anonymous reviewers for AUC Geographica, which helped shape the manuscript in its final form.

References

Afrifa, F. O. T., and Coauthors (2025): A Case Study of Cold-Season Emergent Orographic Convection and Its Impact on Precipitation. Part I: Mesoscale Analysis. Monthly Weather Review 153 (10), 2229–2250, https://doi.org/10.1175/MWR-D-24-0241.1.

American Meteorological Society (AMS) (2025): Cumulonimbus. Glossary of Meteorology. Available online: https://glossary.ametsoc.org/wiki/Cumulonimbus (accessed on 10 November 2025).

Ammon, M. B., Bell, T. M., Smith, E. N., Gebauer, J. G., Pardun, T. J. (2025): Relating the Effects of Heterogeneous Terrain on Boundary-Layer Flow to the Evolution of Preconvection Environments Using Remote Profiler Datasets from PERiLS. Monthly Weather Review 153(11), 2555–2569, https://doi.org/10.1175/MWR-D-24-0108.1.

Bačová Mitková, V., Pekárová, P., Halmová, D., Miklánek, P. (2018): Reconstruction and post-event analysis of a flash flood in a small ungauged basin: a case study in Slovak territory. Natural Hazards 92, 741–760, https://doi.org/10.1007/s11069-018-3222-2.

Banta, R. M. (1990): The Role of Mountain Flows in Making Clouds. In Blumen, W. (Eds.), Atmospheric Processes over Complex Terrain. Meteorological Monographs 23; American Meteorological Society: Boston, MA, https://doi.org/10.1007/978-1-935704-25-6_9.

Barrett, A. I., Gray, S. L., Kirshbaum, D. J., Roberts, N. M., Schultz, D. M., Fairman, J. G., Jr. (2015): Synoptic versus orographic control on stationary convective banding. Quarterly Journal of the Royal Meteorological Society 141(689), 1101–1113, https://doi.org/10.1002/qj.2409.

Barry, R. G. (2008): Mountain Weather and Climate. 3rd ed.; Cambridge University Press: Cambridge, UK, 532 pp., https://doi.org/10.1017/CBO9780511754753.

Barthlott, Ch., Corsmeier, U., Meißner, C., Braun, F., Kottmeier, Ch. (2006): The influence of mesoscale circulation systems on triggering convective cells over complex terrain. Atmospheric Research 81(2), 150–175, https://doi.org/10.1016/j.atmosres.2005.11.010.

Barthlott, Ch., Schipper, J. W., Kalthoff, N., Adler, B., Kottmeier, Ch., Blyth, A., Mobbs, S. (2010): Model representation of boundary-layer convergence triggering deep convection over complex terrain: A case study from COPS. Atmospheric Research 95(2–3), 172–185, https://doi.org/10.1016/j.atmosres.2009.09.010.

Barthlott, Ch., Kalthoff, N. (2011): A Numerical Sensitivity Study on the Impact of Soil Moisture on Convection-Related Parameters and Convective Precipitation over Complex Terrain. Journal of the Atmospheric Sciences 68(12), 2971–2987, https://doi.org/10.1175/JAS-D-11-027.1.

Battaglioli, F., Groenemeijer, P., Púčik, T., Taszarek, M., Ulbrich, U., Rust, H. (2023): Modeled Multidecadal Trends of Lightning and (Very) Large Hail in Europe and North America (1950–2021). Journal of Applied Meteorology and Climatology 62(11), 1627–1653, https://doi.org/10.1175/JAMC-D-22-0195.1.

Bergmaier, P. T., Geerts, B. (2015): Characteristics and Synoptic Environment of Drylines Occurring over the Higher Terrain of Southeastern Wyoming. Weather and Forecasting 30(6), 1733–1748, https://doi.org/10.1175/WAF-D-15-0061.1.

Bianco, L., Djalalova, I. V., King, C. W., Wilczak, J. M. (2011): Diurnal Evolution and Annual Variability of Boundary-Layer Height and Its Correlation to Other Meteorological Variables in California's Central Valley. Boundary-Layer Meteorology 140, 491–511, https://doi.org/10.1007/s10546-011-9622-4.

Blumen, W. (Ed.) (1990): Atmospheric Processes over Complex Terrain. 1st ed.; American Meteorological Society: Boston, MA, USA; 323 pp., https://doi.org/10.1007/978-1-935704-25-6.

Bougeault, P., and Coauthors (2001): The MAP Special Observing Period. Bulletin of the American Meteorological Society 82(3), 433–462, https://doi.org/10.1175/1520-0477(2001)082<0433:TMSOP>2.3.CO;2.

Czech meteorological society (CMeS) (2025): Convective storm (in Czech). Electronic Glossary of Meteorology (eMS). Available online: http://slovnik.cmes.cz/fulltext/317 (accessed on 10 November 2025).

Brooks, H. E., and Coauthors (2019): A Century of Progress in Severe Convective Storm Research and Forecasting. Meteorological Monographs 59(1), 18.1–18.41, https://doi.org/10.1175/AMSMONOGRAPHS-D-18-0026.1.

Czernecki, B., Taszarek, M., Szuster, P. (2025): thundeR: Computation and Visualisation of Atmospheric Convective Parameters. R package version 1.1.3. Available online: https://bczernecki.github.io/thundeR/ (accessed on 10 November 2025).

Da Silva, N. A., Haerter, J. O. (2023): The Precipitation Characteristics of Mesoscale Convective Systems Over Europe. Journal of Geophysical Research: Atmospheres 128(23): e2023JD039045, https://doi.org/10.1029/2023JD039045.

Damiani, R., Zehnder, J., Geerts, B., Demko, J., Haimov, S., Petti, J., Poulos, G. S., Razdan, A., Hu, J., Leuthold, M., French, J. (2008): The Cumulus, Photogrammetric, In Situ, and Doppler Observations Experiment of 2006. Bulletin of the American Meteorological Society 89(1), 57–74, https://doi.org/10.1175/BAMS-89-1-57.

Davolio, S., Volonté, A., Manzato, A., Pucillo, A., Sicogna, A., Ferrario, M. E. (2016): Mechanisms producing different precipitation patterns over north-eastern Italy: Insights from HyMeX-SOP1 and previous events. Quarterly Journal of the Royal Meteorological Society 142(S1), 188–205, https://doi.org/10.1002/qj.2731.

De Wekker, S. F. J., Zhong, S., Fast, D., Whiteman, C. D. (1998): A Numerical Study of the Thermally Driven Plain-to-Basin Wind over Idealized Basin Topographies. Journal of Applied Meteorology and Climatology 37(6), 602–622, https://doi.org/10.1175/1520-0450(1998)037<0606:ANSOTT>2.0.CO;2.

De Wekker, S. F. J., Kossmann, M. (2015): Convective Boundary Layer Heights Over Mountainous Terrain – A Review of Concepts. Frontiers in Earth Science 3: 77, https://doi.org/10.3389/feart.2015.00077.

De Wekker, S. F. J., Kossmann, M., Knievel, J. C., Giovannini, L., Gutmann, E. D., Zardi, D. (2018): Meteorological Applications Benefiting from an Improved Understanding of Atmospheric Exchange Processes over Mountains. Atmosphere 9(10): 371, https://doi.org/10.3390/atmos9100371.

Degiacomi, T., Zonato, A., Davolio, S., Miglietta, M. M., Giovannini, L. (2025): Deep Banded Orographic Convection over an Idealized Mountain Range: Influence of Upstream Atmospheric Conditions. Journal of the Atmospheric Sciences 82(6), 1033–1055, https://doi.org/10.1175/JAS-D-24-0056.1.

Doswell, C. A. (1987): The Distinction between Large-Scale and Mesoscale Contribution to Severe Convection: A Case Study Example. Weather and Forecasting 2(1), 3–16, https://doi.org/10.1175/1520-0434(1987)002<0003:TDBLSA>2.0.CO;2.

Doswell, C. A., Brooks, H. E., Maddox, R. A. (1996): Flash Flood Forecasting: An Ingredients-Based Methodology. Weather and Forecasting 11(4), 560–581, https://doi.org/10.1175/1520-0434(1996)011<0560:FFFAIB>2.0.CO;2.

Doswell, C. A. (2001): Severe Convective Storms – An Overview. Meteorological Monographs 28(50), 1–26, https://doi.org/10.1175/0065-9401-28.50.1.

Doswell, C. A., Bosart, L. F. (2001): Extratropical Synoptic-Scale Processes and Severe Convection. Meteorological Monographs 28(50), 27–70, https://doi.org/10.1175/0065-9401-28.50.27.

Doswell, C. A. (2015): Severe convective storms in the European societal context. Atmospheric Research 158–159, 210–215, https://doi.org/10.1016/j.atmosres.2014.08.007.

Feldmann, M., Germann, U., Gabella, M., Berne, A. (2021): A characterisation of Alpine mesocyclone occurrence. Weather Climate Dynamics 2(4), 1225–1244, https://doi.org/10.5194/wcd-2-1225-2021.

Feldmann, M., Rotunno, R., Germann, U., Berne, A. (2024): Supercell Thunderstorms in Complex Topography – How Mountain Valleys with Lakes Can Increase Occurrence Frequency. Monthly Weather Review 152(2), 471–489, https://doi.org/10.1175/MWR-D-22-0350.1.

Feng, Z., Varble, A., Hardin, J., Marquis, J., Hunzinger, A., Zhang, Z., Thieman, M. (2022): Deep Convection Initiation, Growth, and Environments in the Complex Terrain of Central Argentina during CACTI. Monthly Weather Review 150(5), 1135–1155, https://doi.org/10.1175/MWR-D-21-0237.1.

Fischer, J., Groenemeijer, P., Holzer, A., Feldmann, M., Schröer, K., Battaglioli, F., Schielicke, L., Púčik, T., Antonescu, B., Gatzen, C., TIM Partners (2025): Invited perspectives: Thunderstorm intensification from mountains to plains. Natural Hazards and Earth System Sciences 25(8), 2629–2656, https://doi.org/10.5194/nhess-25-2629-2025.

Frame, J., Markowski, P. (2006): The Interaction of Simulated Squall Lines with Idealized Mountain Ridges. Monthly Weather Review 134(7), 1919–1941, https://doi.org/10.1175/MWR3157.1.

Friedrich, K., Kalina, E. A., Aikins, J., Gochis, D., Rasmussen, R. (2016): Precipitation and Cloud Structures of Intense Rain during the 2013 Great Colorado Flood. Journal of Hydrometeorology 17(1), 27–52, https://doi.org/10.1175/JHM-D-14-0157.1.

Graf, M., Kossmann, M., Trusilova, K., Mühlbacher, G. (2016): Identification and Climatology of Alpine Pumping from a Regional Climate Simulation. Frontiers in Earth Science 4: 5, https://doi.org/10.3389/feart.2016.00005.

Groenemeijer, P., Púčik, T., Holzer, A. M., Antonescu, B., Riemann-Campe, K., Schultz, D. M., Kühne, T., Feuerstein, B., Brooks, H. E., Doswell, C. A., III, Koppert, H., Sausen, R. (2017): Severe Convective Storms in Europe: Ten

Years of Research and Education at the European Severe Storms Laboratory. Bulletin of the American Meteorological Society 98(12), 2641–2651, https://doi.org/10.1175/BAMS-D-16-0067.1.

Hagen, M., van Baelen, J., Richard, E. (2011): Influence of the wind profile on the initiation of convection in mountainous terrain. Quarterly Journal of the Royal Meteorological Society 137(S1), 224–235, https://doi.org/10.1002/qj.784.

Hassanzadeh, H., Schmidli, J., Langhans, W., Schlemmer, L., Schär, C. (2016): Impact of topography on the diurnal cycle of summertime moist convection in idealized simulations. Meteorologische Zeitschrift 25(2), 181–194, https://doi.org/10.1127/metz/2015/0653.

Hilel Goldshmid, R., Bardoel, S. L., Hocut, C. M., Zhong, Q., Liberzon, D., Fernando, H. J. S. (2018): Separation of Upslope Flow over a Plateau. Atmosphere 9(5): 165, https://doi.org/10.3390/atmos9050165.

Houze, R. A., Jr. (1993): Cloud Dynamics; Academic Press: San Diego, USA; 573 pp.

Houze, R. A., Jr., Schmid, W., Fovell, R. G., Schiesser, H.-H. (1993): Hailstorms in Switzerland: Left Movers, Right Movers, and False Hooks. Monthly Weather Review 121(12), 3345–3370, https://doi.org/10.1175/1520-0493(1993)121<3345:HISLMR>2.0.CO;2.

Houze, R. A., Jr. (2012): Orographic effects on precipitating clouds. Reviews of Geophysics 50 (1): RG1001, https://doi.org/10.1029/2011RG000365.

Chen, S., Lin, Y. (2005): Effects of Moist Froude Number and CAPE on a Conditionally Unstable Flow over a Mesoscale Mountain Ridge. Journal of the Atmospheric Sciences 62(2), 331–350, https://doi.org/10.1175/JAS-3380.1.

Chow, F. K., De Wekker, S. F. J., Snyder, B. J. (2013): Mountain Weather Research and Forecasting: Recent Progress and Current Challenges; Springer: Dordrecht, Netherlands; 750 pp., https://doi.org/10.1007/978-94-007-4098-3.

Chu, C., Lin, Y. (2000): Effects of orography on the generation and propagation of mesoscale convective systems in a two-dimensional conditionally unstable flow. Journal of the Atmospheric Sciences 57(23), 3817–3837, https://doi.org/10.1175/1520-0469(2001)057<3817:EOOOTG>2.0.CO;2.

Imamovic, A., Schlemmer, L., Schär, C. (2017): Collective Impacts of Orography and Soil Moisture on the Soil Moisture-Precipitation Feedback. Geophysical Research Letters 44(22), 11682–11691, https://doi.org/10.1002/2017GL075657.

Imamovic, A., Schlemmer, L., Schär, C. (2019): Mountain Volume Control on Deep-Convective Rain Amount during Episodes of Weak Synoptic Forcing. Journal of the Atmospheric Sciences 76(2), 605–626, https://doi.org/10.1175/JAS-D-18-0217.1.

Kaltenboeck, R., Steinheimer, M. (2015): Radar-based severe storm climatology for Austrian complex orography related to vertical wind shear and atmospheric instability. Atmospheric Research 158–159, 216–230, https://doi.org/10.1016/j.atmosres.2014.08.006.

Kalthoff, N., Kohler, M., Barthlott, C., Adler, B., Mobbs, S. D., Corsmeier, U., Traumner, K., Foken, T., Eigenmann, R., Krauss, L., and Coauthors (2011): The dependence of convection-related parameters on surface and boundary-layer conditions over complex terrain. Quarterly Journal of the Royal Meteorological Society 137(S1), 70–80, https://doi.org/10.1002/qj.686.

Kang, S.-L., Ryu, J.-H. (2016): Response of moist convection to multi-scale surface flux heterogeneity. Quarterly Journal of the Royal Meteorological Society 142(698), 2180–2193, https://doi.org/10.1002/qj.2811.

Kaspar, M., Müller, M., Kakos, V., Řezáčová, D., Sokol, Z. (2009): Severe storm in Bavaria, the Czech Republic and Poland on 12–13 July 1984: A statistic- and model-based analysis. Atmospheric Research 93(1–3), 99–110, https://doi.org/10.1016/j.atmosres.2008.10.004.

Kašpar, M., Bližňák, V., Hulec, F., Müller, M. (2021): High-resolution spatial analysis of the variability in the subdaily rainfall time structure. Atmospheric Research 248: 105202, https://doi.org/10.1016/j.atmosres.2020.105202.

Katona, B., Markowski, P., Alexander, C., Benjamin, S. (2016): The Influence of Topography on Convective Storm Environments in the Eastern United States as Deduced from the HRRR. Weather and Forecasting 31(5), 1481–1490, https://doi.org/10.1175/WAF-D-16-0038.1.

Kelsey, E., Bailey, A., Murray, G. (2018): The Impact of Mount Washington on the Height of the Boundary Layer and the Vertical Structure of Temperature and Moisture. Atmosphere 9(8): 293, https://doi.org/10.3390/atmos9080293.

Khodayar, S., Kalthoff, N., Wickert, J., Kottmeier, Ch., Dorninger, M. (2013): High-resolution representation of the mechanisms responsible for the initiation of isolated thunderstorms over flat and complex terrains: analysis of CSIP and COPS cases. Meteorology and Atmospheric Physics 119, 109–124, https://doi.org/10.1007/s00703-012-0232-6.

Kirshbaum, D. J., Bryan, G. H., Rotunno, R., Durran, D. R. (2007): The Triggering of Orographic Rainbands by Small-Scale Topography. Journal of the Atmospheric Sciences 64(5), 1530–1549, https://doi.org/10.1175/JAS3924.1.

Kirshbaum, D. J. (2013): On Thermally Forced Circulations over Heated Terrain. Journal of the Atmospheric Sciences 70(6), 1690–1709, https://doi.org/10.1175/JAS-D-12-0199.1.

Kirshbaum, D. J., Wang, C. (2014): Boundary Layer Updrafts Driven by Airflow over Heated Terrain. Journal of the Atmospheric Sciences 71(4), 1425–1442, https://doi.org/10.1175/JAS-D-13-0287.1.

Kirshbaum, D. J., Fabry, F. Cazenave, Q. (2016): The Mississippi Valley Convection Minimum on Summer Afternoons: Observations and Numerical Simulations. Monthly Weather Review 144(1), 263–272, https://doi.org/10.1175/MWR-D-15-0238.1.

Kirshbaum, D. J. (2017): On upstream blocking over heated mountain ridges. Quarterly Journal of the Royal Meteorological Society 143(702), 53–68, https://doi.org/10.1002/qj.2945.

Kirshbaum, D. J., Schultz, D. M. (2018): Convective Cloud Bands Downwind of Mesoscale Mountain Ridges. Journal of the Atmospheric Sciences 75(12), 4265–4286, https://doi.org/10.1175/JAS-D-18-0211.1.

Kirshbaum, D. J., Adler, B., Kalthoff, N., Barthlott, Ch., Serafin, S. (2018): Moist Orographic Convection: Physical Mechanisms and Links to Surface-Exchange Processes. Atmosphere 9(3): 80, https://doi.org/10.3390/atmos9030080.

Kottmeier, C., Kalthoff, N., Barthlott, C., Corsmeier, U., van Baelen, J., Behrendt, A., Behrendt, R., Adler, B., Blyth, A., Coulter, R., Crewell, S., di Girolamo, P., Dorninger, M., Flamant, C., Foken, T., Gorgas, T., Harnisch, F., Hauck, C., Höller, H., Konow, H., Kunz, M., Mahalek, H., Mobbs, S., Richard, E., Steinacker, R., Weckwerth, T., Wieser, A., Wulfmeyer, V. (2008): Mechanisms initiating deep convection over complex terrain during COPS. Meteorologische Zeitschrift 17(6), 931–948, https://doi.org/10.1127/0941-2948/2008/0348.

Kühne, T., Antonescu, B., Groenemeijer, P., Púčik, T. (2025): Lightning Fatalities in Europe (2001–20). Weather, Climate, and Society 17(2), 205–215, https://doi.org/10.1175/WCAS-D-24-0038.1.

Kunz, M., Blahak, U., Handwerker, J., Schmidberger, M., Punge, H. J., Mohr, S., Fluck, E., Bedka, K. M. (2018): The severe hailstorm in southwest Germany on 28 July 2013: characteristics, impacts and meteorological conditions. Quarterly Journal of the Royal Meteorological Society 144(710), 231–250, https://doi.org/10.1002/qj.3197.

Kvak, R., Okon, Ľ., Bližňák, V., Méri, L., Kašpar, M. (2023): Spatial distribution and precipitation intensity of supercells: Response to terrain asymmetry in the Western Carpathians, Central Europe. Atmospheric Research 292: 106885, https://doi.org/10.1016/j.atmosres.2023.106885.

Laiti, L., Zardi, D., de Franceschi, M., Rampanelli, G., Giovannini, L. (2014): Analysis of the diurnal development of a lake-valley circulation in the Alps based on airborne and surface measurements. Atmospheric Chemistry and Physics 14(18), 9771–9786, https://doi.org/10.5194/acp-14-9771-2014.

Lareau, N. P., Knopp, T., Kirshbaum, D. J. (2024): Mechanical and Thermal Forcing for Upslope Flows and Cumulus Convection over the Sierras de Córdoba. Monthly Weather Review 152(9), 2149–2167, https://doi.org/10.1175/MWR-D-23-0254.1.

Levizzani, V., Pinelli, F., Pasqui, M., Melani, S., Laing, A. G., Carbone, R. E. (2010): A 10-year climatology of warm-season cloud patterns over Europe and the Mediterranean from Meteosat IR observations. Atmospheric Research 97(4), 555–576, https://doi.org/10.1016/j.atmosres.2010.05.014.

Lock, N. A., Houston, A. L. (2014): Empirical Examination of the Factors Regulating Thunderstorm Initiation. Monthly Weather Review 142(1), 240–258, https://doi.org/10.1175/MWR-D-13-00082.1.

Lock, N. A., Houston, A. L. (2015): Spatiotemporal distribution of thunderstorm initiation in the US Great Plains from 2005 to 2007. International Journal of Climatology 35(13), 4047–4056, https://doi.org/10.1002/joc.4261.

Lombardo, K., Bitting, M. (2024): A Climatology of Convective Precipitation over Europe. Monthly Weather Review 152(7), 1555–1585, https://doi.org/10.1175/MWR-D-23-0156.1.

Marquis, J. N., Varble, A. C., Robinson, P., Nelson, T. C., Friedrich, K. (2021): Low-Level Mesoscale and Cloud-Scale Interactions Promoting Deep Convection Initiation. Monthly Weather Review 149(8), 2473–2495, https://doi.org/10.1175/MWR-D-20-0391.1.

Marquis, J. N., Feng, Z., Varble, A., Nelson, T. C., Houston, A., Peters, J. M., Mulholland, J. P., Hardin, J. (2023): Near-Cloud Atmospheric Ingredients for Deep Convection Initiation. Monthly Weather Review 151(5), 1247–1267, https://doi.org/10.1175/MWR-D-22-0243.1.

Markowski, P., Richardson, Y. (2010): Mesoscale Meteorology in Midlatitudes; Wiley-Blackwell: Chichester, UK, and Hoboken, NJ, USA; 407 pp., http://dx.doi.org/10.1002/9780470682104.

Markowski, P., Dotzek, N. (2011): A numerical study of the effects of orography on supercells. Atmospheric Research 100(4), 457–478, https://doi.org/10.1016/j.atmosres.2010.12.027.

McKeown, K. E., Davenport, C. E., Eastin, M. D., Purpura, S. M., Riggin, R. R. (2024): Radar Characteristics of Supercell Thunderstorms Traversing the Appalachian Mountains. Weather and Forecasting 39(4), 639–654, https://doi.org/10.1175/WAF-D-23-0110.1.

Miglietta, M. M., Rotunno, R. (2014): Numerical Simulations of Sheared Conditionally Unstable Flows over a Mountain Ridge. Journal of the Atmospheric Sciences 71(5), 1747–1762, https://doi.org/10.1175/JAS-D-13-0297.1.

Mulholland, J. P., Nesbitt, S. W., Trapp, R. J., Rasmussen, K. L., Salio, P. V. (2018): Convective Storm Life Cycle and Environments near the Sierras de Córdoba, Argentina. Monthly Weather Review 146(8), 2541–2557, https://doi.org/10.1175/MWR-D-18-0081.1.

Mulholland, J. P., Nesbitt, S. W., Trapp, R. J. (2019): A Case Study of Terrain Influences on Upscale Convective Growth of a Supercell. Monthly Weather Review 147(12), 4305–4324, https://doi.org/10.1175/MWR-D-19-0099.1.

Mulholland, J. P., Nesbitt, S. W., Trapp, R. J., Peters, J. M. (2020): The Influence of Terrain on the Convective Environment and Associated Convective Morphology from an Idealized Modeling Perspective. Journal of the Atmospheric Sciences 77(11), 3929–3949, https://doi.org/10.1175/JAS-D-19-0190.1.

Nelson, T. C., Marquis, J., Varble, A., Friedrich, K. (2021): Radiosonde Observations of Environments Supporting Deep Moist Convection Initiation during RELAMPAGO-CACTI. Monthly Weather Review 149(1), 289–309, https://doi.org/10.1175/MWR-D-20-0148.1.

Nelson, T. C., Marquis, J., Peters, J. M., Friedrich, K. (2022): Environmental Controls on Simulated Deep Moist Convection Initiation Occurring during RELAMPAGO-CACTI. Journal of the Atmospheric Sciences 79(7), 1941–1964, https://doi.org/10.1175/JAS-D-21-0226.1.

Nicolas, Q., Boos, W. R. (2022): A Theory for the Response of Tropical Moist Convection to Mechanical Orographic Forcing. Journal of the Atmospheric Sciences 79(7), 1761–1779, https://doi.org/10.1175/JAS-D-21-0218.1.

Panosetti, D., Boing, S., Schlemmer, L., Schmidli, J. (2016): Idealized Large-Eddy and Convection-Resolving Simulations of Moist Convection over Mountainous Terrain. Journal of the Atmospheric Sciences 73(10), 4021–4041, https://doi.org/10.1175/JAS-D-15-0341.1.

Panziera, L., James, C. N., Germann, U. (2015): Mesoscale Organization and Structure of Orographic Precipitation Producing Flash Floods in the Lago Maggiore Region. Quarterly Journal of the Royal Meteorological Society 141(686), 224–248, https://doi.org/10.1002/qj.2351.

Panziera, L., Gabella, M., Germann, U., Martius, O. (2018): A 12-year radar-based climatology of daily and sub-daily extreme precipitation over the Swiss Alps. International

Journal of Climatology 38(10), 3749–3769, https://doi.org/10.1002/joc.5528.
Peterson, D. A., Fromm, M. D., Solbrig, J. E., Hyer, E. J., Surratt, M. L., Campbell, J. R. (2017): Detection and Inventory of Intense Pyroconvection in Western North America using GOES-15 Daytime Infrared Data. Journal of Applied Meteorology and Climatology 56(2), 471–493, https://doi.org/10.1175/JAMC-D-16-0226.1.
Peterson, M., Mach, D., Buechler, D. (2021): A Global LIS/OTD Climatology of Lightning Flash Extent Density. Journal of Geophysical Research: Atmospheres 126(8): e2020JD033885, https://doi.org/10.1029/2020JD033885.
Price, M. F., Arnesen, T., Gløersen, E., Metzger, M. J. (2019): Mapping mountain areas: learning from Global, European and Norwegian perspectives. Journal of Mountain Science 16, 1–15, https://doi.org/10.1007/s11629-018-4916-3.
Punge, H. J., Kunz, M. (2016): Hail observations and hailstorm characteristics in Europe: A review. Atmospheric Research 176–177, 159–184, https://doi.org/10.1016/j.atmosres.2016.02.012.
Purpura, S. M., Davenport, C. E., Eastin, M. D., McKeown, K. E., Riggin, R. R. (2023): Environmental Evolution of Supercell Thunderstorms Interacting with the Appalachian Mountains. Weather and Forecasting 38(1), 179–198, https://doi.org/10.1175/WAF-D-22-0115.1.
Púčik, T., Groenemeijer, P., Rýva, D., Kolář, M. (2015): Proximity Soundings of Severe and Nonsevere Thunderstorms in Central Europe. Monthly Weather Review 143(12), 4805–4821, https://doi:10.1175/MWR-D-15-0104.1.
Reeves, H. D., Lin, Y.-L. (2007): The Effects of a Mountain on the Propagation of a Preexisting Convective System for Blocked and Unblocked Flow Regimes. Journal of the Atmospheric Sciences 64(7), 2401–2421, https://doi.org/10.1175/JAS3959.1.
Reif, D. W., Bluestein, H. B. (2018): Initiation Mechanisms of Nocturnal Convection without Nearby Surface Boundaries over the Central and Southern Great Plains during the Warm Season. Monthly Weather Review 146(9), 3053–3078, https://doi.org/10.1175/MWR-D-18-0040.1.
Řezáčová, D., Novák, P., Kašpar, M., Setvák, M. (2007): The Physics of Clouds and Precipitation (in Czech); Academia: Praha, Czech Republic, 574 pp.
Ribeiro, B. Z., Bosart, L. F. (2018): Elevated Mixed Layers and Associated Severe Thunderstorm Environments in South and North America. Monthly Weather Review 146(1), 3–28, https://doi.org/10.1175/MWR-D-17-0121.1.
Roe, G. H. (2005): Orographic precipitation. Annual Review of Earth and Planetary Sciences 33, 645–671, https://doi.org/10.1146/annurev.earth.33.092203.122541.
Rorig, M. L., Ferguson, S. A. (1999): Characteristics of Lightning and Wildland Fire Ignition in the Pacific Northwest. Journal of Applied Meteorology and Climatology 38(11), 1565–1575, https://doi.org/10.1175/1520-0450(1999)038<1565:COLAWF>2.0.CO;2.
Rotach, M. W., Serafin, S., Ward, H. C., Arpagaus, M., Colfescu, I., Cuxart, J., De Wekker, S. F. J., Grubišić, V., Kalthoff, N., Karl, T., Kirshbaum, D. J., Lehner, M., Mobbs, S., Paci, A., Palazzi, E., Bailey, A., Schmidli, J., Wittmann, C., Wohlfahrt, G., Zardi, D. (2022): A Collaborative Effort to Better Understand, Measure, and Model Atmospheric Exchange Processes over Mountains. Bulletin of the American Meteorological Society 103(5), E1282–E1295, https://doi.org/10.1175/BAMS-D-21-0232.1.
Scheffknecht, P., Serafin, S., Grubišić, V. (2017): A long-lived supercell over mountainous terrain. Quarterly Journal of the Royal Meteorological Society 143(709), 2973–2986, https://doi.org/10.1002/qj.3127.
Schmidli, J., Rotunno, R. (2012): Influence of the valley surroundings on valley wind dynamics. Journal of the Atmospheric Sciences 69(2), 561–577, https://doi.org/10.1175/JAS-D-11-0129.1.
Schneider, L., Barthlott, C., Barrett, A., Hoose, C. (2018): The precipitation response to variable terrain forcing over low-mountain ranges in different weather regimes. Quarterly Journal of the Royal Meteorological Society 144(713), 970–989, https://doi.org/10.1002/qj.3250.
Serafin, S., Zardi, D. (2010): Daytime Heat Transfer Processes Related to Slope Flows and Turbulent Convection in an Idealized Mountain Valley. Journal of the Atmospheric Sciences 67(11), 3739–3756, https://doi.org/10.1175/2010JAS3428.1.
Serafin, S., Adler, B., Cuxart, J., De Wekker, S. F. J., Gohm, A., Grisogono, B., Kalthoff, N., Kirshbaum, D. J., Rotach, M. W., Schmidli, J., Stiperski, I., Večenaj, Ž., Zardi, D. (2018): Exchange Processes in the Atmospheric Boundary Layer Over Mountainous Terrain. Atmosphere 9(3): 102, https://doi.org/10.3390/atmos9030102.
Singh, I., Nesbitt, S. W., Davis, C. A. (2022): Quasi-Idealized Numerical Simulations of Processes Involved in Orogenic Convection Initiation over the Sierras de Córdoba. Journal of the Atmospheric Sciences 79(4), 1127–1149, https://doi.org/10.1175/JAS-D-21-0007.1.
Schultz, D. M., Young, M. V., Kirshbaum, D. J. (2025): The Spanish Plume Elevated Mixed Layer: A Review of Its Use and Misuse within the Scientific Literature. Monthly Weather Review 153(5), 737–761, https://doi.org/10.1175/MWR-D-24-0139.1.
Smith, V. H., Mobbs, S. D., Burton, R. R., Hobby, M., Aoshima, F., Wulfmeyer, V., Di Girolamo, P. (2015): The role of orography in the regeneration of convection: A case study from the convective and orographically-induced precipitation study. Meteorologische Zeitschrift 24(1), 83–97, https://doi.org/10.1127/metz/2014/0418.
Soderholm, B., Ronalds, B., Kirshbaum, D. J. (2014): The Evolution of Convective Storms Initiated by an Isolated Mountain Ridge. Monthly Weather Review 142(4), 1430–1451, https://doi.org/10.1175/MWR-D-13-00280.1.
Tang, B., Vaughan, M., Lazear, R., Corbosiero, K., Bosart, L., Wasula, T., Lee, I., Lipton, K. (2016): Topographic and Boundary Influences on the 22 May 2014 Duanesburg, New York, Tornadic Supercell. Weather and Forecasting 31(1), 107–127, https://doi.org/10.1175/WAF-D-15-0101.1.
Taszarek, M., Allen, J. T., Púčik, T., Groenemeijer, P., Czernecki, B., Kolendowicz, L., Lagouvardos, K., Kotroni, V., Schulz, W. (2019): A Climatology of Thunderstorms across Europe from a Synthesis of Multiple Data Sources. Journal of Climate 32(6), 1813–1837, https://doi.org/10.1175/JCLI-D-18-0372.1.
Taszarek, M., Allen, J. T., Groenemeijer, P., Edwards, R., Brooks, H. E., Chmielewski, V., Enno, S.-E. (2020a): Severe

Convective Storms across Europe and the United States. Part I: Climatology of Lightning, Large Hail, Severe Wind, and Tornadoes. Journal of Climate 33(23), 10239–10261, https://doi.org/10.1175/JCLI-D-20-0345.1.

Taszarek, M., Allen, J. T., Púčik, T., Hoogewind, K. A., Brooks, H. E. (2020b): Severe Convective Storms across Europe and the United States. Part II: ERA5 Environments Associated with Lightning, Large Hail, Severe Wind, and Tornadoes. Journal of Climate 33(23), 10263–10286, https://doi.org/10.1175/JCLI-D-20-0346.1.

Trefalt, S., Martynov, A., Barras, H., Besic, N., Hering, A. M., Lenggenhager, S., Noti, P., Röthlisberger, M., Schemm, S., Germann, U., Martius, O. (2018): A severe hail storm in complex topography in Switzerland – observations and processes. Atmospheric Research 209, 76–94, https://doi.org/10.1016/j.atmosres.2018.03.007.

Wagner, J. S., Gohm, A., Rotach, M. W. (2015): The impact of valley geometry on daytime thermally driven flows and vertical transport processes. Quarterly Journal of the Royal Meteorological Society 141(690), 1780–1794, https://doi.org/10.1002/qj.2481.

Wang, Q. W., Xue, M., Tan, Z. M. (2016): Convective initiation by topographically induced convergence forcing over the Dabie Mountains on 24 June 2010. Advances in Atmospheric Sciences 33(10), 1120–1136, https://doi.org/10.1007/s00376-016-6024-z.

Weckwerth, T. M., Wilson, J. W., Hagen, M., Emerson, T. J., Pinto, J. O., Rife, D. L., Grebe, L. (2011): Radar climatology of the COPS region. Quarterly Journal of the Royal Meteorological Society 137(S1), 31–41, https://doi.org/10.1002/qj.747.

Weckwerth, T. M., Bennett, L. J., Jay Miller, L., Van Baelen, J., Di Girolamo, P., Blyth, A. M., Hertneky, T. J. (2014): An Observational and Modeling Study of the Processes Leading to Deep, Moist Convection in Complex Terrain. Monthly Weather Review 142(8), 2687–2708, https://doi.org/10.1175/MWR-D-13-00216.1.

Weisman, M. L., Klemp, J. B. (1982): The Dependence of Numerically Simulated Convective Storms on Vertical Wind Shear and Buoyancy. Monthly Weather Review 110(6), 504–520, https://doi.org/10.1175/1520-0493(1982)110<0504:TDONSC>2.0.CO;2.

Whiteman, C. D. (2000): Mountain Meteorology: Fundamentals and Applications; Oxford University Press: New York, NY, USA; 355 pp., https://doi.org/10.1093/oso/9780195132717.001.0001.

Wulfmeyer, V., and Coauthors (2011): The Convective and Orographically-induced Precipitation Study (COPS): the scientific strategy, the field phase, and research highlights. Quarterly Journal of the Royal Meteorological Society 137(S1), 3–30, https://doi.org/10.1002/qj.752.